Stony Brook University

Does Lunatic Fringe modify itself?

A Thesis Presented

by

Usman Aslam

to

The Graduate School

in Partial Fulfillment of the

Requirements

for the Degree of

Master of Science

in

Biochemistry and Cell Biology

Stony Brook University

December 2013

Stony Brook University

The Graduate School

Usman Aslam

We, the thesis committee for the above candidate for the

Master of Science degree, hereby recommend

acceptance of this thesis.

Robert S. Haltiwanger – Thesis Advisor
Professor and Chair
Department of Biochemistry and Cell Biology

Harvard Lyman– Second Reader
Associate Professor
Department of Biochemistry and Cell Biology

This thesis is accepted by the Graduate School

Charles Taber
Dean of the Graduate School

Abstract of the Thesis

Does Lunatic Fringe modify itself?

by

Usman Aslam

Master of Science

in

Biochemistry and Cell Biology

Stony Brook University

2013

Notch signaling plays an essential role in metazoan development, and dysregulation of its activity has been recognized as a cause for many diseases. The extracellular domain of the Notch receptor has numerous tandem epidermal growth factor-like repeats modified with *O*-fucose and *O*-glucose glycans that play important roles in Notch function. Elongation of *O*-fucose by β3-*N*-acetylglucosaminyltransferases of the Fringe family is known to modulate Notch activity. In addition, preliminary data from the Haltiwanger laboratory suggests that one of the Fringe enzymes, Lunatic Fringe, may modify itself. Lunatic Fringe does not contain any epidermal growth factor-like repeats and is not known to be modified by *O*-fucose, but it is modified with an *N*-linked glycan that may contain fucose. Our hypothesis is that Lunatic Fringe may modify itself on a fucose linked to an *N*-glycan. The goal of this project is to characterize the structure of the *N*-linked glycans attached to Lunatic Fringe and to further examine the self-modification of Lunatic Fringe.

Table of Contents

List of Figures……...……...v
List of Abbreviations……...……...……..……..……vii
Acknowledgements……..……...ix

I. INTRODUCTION……1
II. MATERIAL AND METHODS……5
III. RESULTS……...8
IV. DISCUSSION……..……12
V. FIGURES……..….19
REFERENCES……...……..41

List of Figures

Figure 1 (pg. 19): Schematic representation of the extracellular domain of mouse Notch 1.

Figure 2 (pg. 20): Notch activation pathway.

Figure 3 (pg. 21): Epidermal growth factor-like repeat found on mN1.

Figure 4A (pg. 22): Biosynthesis of *N*-linked glycan core through modification of Dolichol-phosphate.

Figure 4B (pg. 23): Common types of *N*-linked glycans.

Figure 4C (pg. 24): Maturation of *N*-linked glycans.

Figure 5 (pg. 25): Peptide-*N*-Glycosidase F (PNGase F) cleavage sites.

Figure 6 (pg. 26): Flowchart of PVDF glycomics method (A) and of Western PVDF glycomics method (B).

Figure 7A (pg. 27): Structure of pure $Man_9GlcNAc_2$ standard glycan used to test effectiveness of PGC chip linked LC/MS apparatus.

Figure 7B (pg. 27): Base peak chromatogram (BPC) of $Man_9GlcNAc_2$ standard glycan produced from 530 femtomoles of sample.

Figure 7C (pg. 27): MS of parent peak with a mass-to-charge ratio of 942.8, observed at approximately 4.6 minutes.

Figure 7D (pg. 28): MS/MS fragmentation pattern of parent peak with mass-to-charge ratio of 942.8 observed at approximately 4.6 minutes.

Figure 7E (pg. 28): MS of parent peak with a mass-to-charge ratio of 942.9, observed at approximately 5.0 minutes.

Figure 7F (pg. 29): MS/MS fragmentation pattern of parent peak with mass-to-charge ratio of 942.9 observed at approximately 5.0 minutes.

Figure 8A (pg. 29): Known *N*-linked glycan structure has a molecular weight of 1462.53 Daltons.

Figure 8B (pg. 29): Base peak chromatogram of purified IgG *N*¬-linked glycan.

Figure 8C (pg. 30): EIC of a mass-to-charge ratio of 732 corresponding to IgG glycan in +2 charge state.

Figure 8D (pg. 30): MS of parent peak with a mass-to-charge ratio of 732.8, observed at approximately 5.5 minutes.

Figure 8E (pg. 31): MS/MS fragmentation pattern of parent peak with mass-to-charge ratio of 733.1 observed at approximately 5.5 minutes.
Figure 8F (pg. 31): MS of parent peak with a mass-to-charge ratio of 732.7, observed at approximately 6.1 minutes.
Figure 8G (pg. 32): MS/MS fragmentation pattern of parent peak with mass-to-charge ratio of 733.2 observed at approximately 6.1 minutes.
Figure 9A (pg. 32): Base peak chromatogram of *N*-linked glycans isolated from Lfng protein grown in Lec1 CHO cells.
Figure 9B (pg. 33): MS of parent peak with a mass-to-charge ratio of 1235.9, observed at approximately 5.6 minutes.
Figure 9C (pg. 33): MS/MS fragmentation pattern of parent peak with mass-to-charge ratio of 1236.2 observed at approximately 5.6 minutes.
Figure 9D (pg. 33): MS of parent peak with a mass-to-charge ratio of 1236.0, observed at approximately 6.2 minutes.
Figure 9E (pg. 34): MS/MS fragmentation pattern of parent peak with mass-to-charge ratio of 1236.2 observed at approximately 6.2 minutes.
Figure 9F (pg. 34): Preliminary Lfng *N*-linked glycan structures.
Figure 9G (pg. 35): Comparison between EIC of preliminary Lfng glycan structure with fucose modification (1381 m/z in the +1 charge state) and EIC of preliminary Lfng glycan structure without fucose modification (1236 m/z in the +1 charge state).
Figure 10A (pg. 36): Flowchart of individual steps taken to complete radioactivity assay.
Figure 10B (pg. 37): Scintillation readings for aliquots of sample collected from size exclusion chromatography of samples with varying radioactivity assay reagents.
Figure 10C (pg. 38): Protein samples, from scintillation counter tests, purified and separated by SDS-PAGE.
Figure 10D (pg. 39): SDS-PAGE gel dried and placed on an undeveloped film for two months.
Figure 10E (pg. 40): Coomassie gel with protein sample (Fig. 10C) with autoradiograph (Fig. 10D) placed on top to reveal identities of radioactive signals.

List of Abbreviations

ADAM	A disintegrin and metalloproteinase
Asn	Asparagine
BPC	Base peak chromatogram
CADASIL	Cerebral Autosomal-Dominant Arteriopathy with Subcortical Infarcts and Leukoencephalopathy
CHO cells	Chinese hamster ovary cells
Cys	Cysteine
Dol	Dolichol
ECD	Extracellular domain
EGF	Epidermal growth factor like
EIC	Extracted ion chromatogram
ER	Endoplasmic reticulum
ESI	Electrospray ionization
Fuc	Fucose
Gal	Galactose
GlcNAc	N-Acetylglucosamine
Glc	Glucose
HEK293T cells	Human embryo kidney 293 cells transformed with SV40 Large T-antigen
HEPES	4-(2-hydroxyethyl)-1-piperazineethanesulfonic acid
His-tag	Poly-histidine tag
HPLC	High performance liquid chromatography
ICD	Intracellular domain
IgG	Immunoglobulin G
kDa	Kilo Dalton
LC	Liquid chromatography
MALDI	Matrix-assisted laser desorption/ ionization
MAN-9	$Man_9GlcNAc_2$ glycan standard
Man	Mannose
Mfng	Manic Fringe

mLfng	Mouse Lunatic Fringe
mN1	Mouse Notch 1
MS	Mass spectrometer
MS/MS	Tandem mass spectrometry
Ni-NTA	Nickel Nitrilotriacetic acid
NP-40	Nonyl phenoxypolyethoxylethanol
PAGE	Polyacrylamide gel electrophoresis
PEI	Polyethylenimine
PGC	Porous graphitized carbon
PNGase F	Peptide N-Glycosidase F
Pofut-1	Protein O-fucosyltransferase 1
PVDF	Polyvinylidene flouride
PVP40	Polyvinylpyrrolidone with molecular weight of 40,000 Daltons
Rfng	Radical Fringe
RPM	Revolutions per minute
SDS	Sodium dodecyl sulfate
Ser	Serine
Thr	Threonine
TSR	Thrombospondin type 1
Tris-HCL	Tris(hydroxymethyl)amino methane hydrochloric acid
Vol	Volume
Wt	Weight

Acknowledgments

I would like to thank my advisor Dr. Robert S. Haltiwanger for introducing me to the vast world of glycobiology and allowing me the opportunity to work in his lab. His guidance and constant encouragements provided me with a valuable platform for intellectual and personal growth.

I thank Rich Grady, Beth Harvey, Shinako Kakuda, Joshua Kantharia, Michael Schneider, Hideyuki Takeuchi, Megumi Takeuchi, and Deepika Vasudevan for their helpful discussions and support in lab. Fundamentally, I thank them for creating a very friendly and enjoyable environment to work in.

I would like to thank my mentor and friend, Esam Al-Shareffi, for guiding me through all aspects of this project and providing me with help any time I needed.

Most importantly, I would like to thank my family. Without their unconditional love and support, none of this would have been possible.

This research was supported by NIH grant GM06112.

I: Introduction

The Notch receptor initiates an evolutionarily conserved cell signaling pathway used by metazoans to control cell fates and a wide array of developmental processes (Artavanis-Tsakonas, Rand et al. 1999). The Notch gene was first identified in *Drosophila melanogaster* as a spontaneous dominant X-linked mutation (Mohr 1919). It is named after the characteristic 'Notch' of tissue loss in the wing blades of animals lacking a functional copy of the Notch gene. Loss of both functional copies of Notch results in lethality through hyperplasia of embryonic nervous system (Dexter 1914, Mohr 1919). The importance of Notch is highlighted by its causative role, through gain and loss of function mutations, in a variety developmental disorders, some of which include Alagille syndrome, spondylocostal dystosis, cerebral autosomal dominant arteriopathy with subcortical dystosis (CADASIL), multiple sclerosis, and some forms of cancer (Jafar-Nejad, Leonardi et al. 2010).

The 300 kDa Notch receptor consists of three basic domains: the extracellular domain (ECD) with 36 tandem epidermal growth factor (EGF) like repeats, a single trans-membrane domain, and an intracellular domain containing several nuclear localization sequences (Fig. 1) (Wharton, Johansen et al. 1985, Rana and Haltiwanger 2011). Signal activation is initiated when the ECD of Notch interacts with members of the DSL family of ligands (Delta, Serrate, or Lag2) on the cell surface of adjacent cells (Fig. 2) (Fortini 2009, Rana and Haltiwanger 2011). The resulting conformational change in Notch allows a disintegrin and metalloprotease (ADAM) on the cell's surface to cleave Notch along the cell membrane (S2 cleavage) (van Tetering, van Diest et al. 2009). Following the S2 cleavage, gamma-secretase catalyzes another cleavage event (S3 cleavage) within the membrane, which results in the release of Notch's intracellular domain (ICD) into the cytoplasm (Schroeter, Kisslinger et al. 1998). The ICD translocates to the nucleus where it modulates transcription of target genes (Fig. 2) (Jarriault, Brou et al. 1995).

Glycan modifications are present abundantly on the ECD of Notch and can modulate signaling activity (Haltiwanger and Lowe 2004). The EGF-like domains, present as tandem repeats on the ECD of Notch (Fig. 1), are characterized by six cysteine residues that form three intra-chain disulfide that result in a distinct folding pattern (Fig. 3) (Rana and Haltiwanger 2011). These EGF-like repeats have unique consensus sequences for O-fucose and O-glucose modifications (Fig. 3) (Rana and Haltiwanger 2011). Addition of O-fucose is catalyzed by

protein O-fucosyltransferase 1 (Pofut-1) in the endoplasmic reticulum (Luo and Haltiwanger 2005). It occurs on Ser/Thr within the consensus sequence C-X-X-X-X-(S/T)-C between the second and third cysteine in EGF repeats (Fig. 3) (Harris and Spellman 1993). This O-fucose can be further elongated by the addition of *N*-acetylglucosamine, Galactose and sialic acid in the Golgi apparatus by Fringe family enzymes (Moloney, Panin et al. 2000). The O-fucose modification plays a vital role in ligand mediated Notch activation as deletion or reduction of Pofut1 levels results in embryonic lethality and phenotypes that are consistent with Notch signaling defects (Shi and Stanley 2003). O-Glucosylation occurs on Ser within the consensus sequence C-X-S-X-P-X between the first and second cysteine conserved in EGF repeats (Takeuchi, Fernandez-Valdivia et al. 2011). Elimination of the enzyme responsible for O-glycosylation, Rumi, also results in severe Notch-like phenotypes (Acar, Jafar-Nejad et al. 2008).

Protein modulators affect the strength of Notch signaling at all levels of the signaling cascade, and the Fringe family of enzymes plays an important role in modulation of Notch activity (Irvine and Wieschaus 1994). This family of highly conserved β1–3*N*-acetylglucosaminyltransferases is present in the Golgi apparatus, and are known to potentiate Notch's ability to interact with its extracellular ligands (Bruckner, Perez et al. 2000). The Fringe enzymes specifically catalyze the transfer of GlcNAc from UDP-GlcNAc to an acceptor fucose creating a disaccharide (Moloney, Panin et al. 2000). Three mammalian Fringe homologues have been identified, Manic Fringe (Mfng), Lunatic Fringe (Lfng), and Radical Fringe (Rfng) (Johnston, Rauskolb et al. 1997). There is evidence that both Lfng and Rfng affect developmental patterns in vertebrates (Rodriguez-Esteban, Scwabe et al. 1997). Mice with disrupted Lfng expression experience severe rib malformation, which leads to perinatal death (Zhang and Gridley 1998). The mice that do survive have malformations in their vertebral column and ribs, fusion of neural arches and shortened tails; these defects are associated with defects in somitogenesis (Zhang and Gridley 1998).

The Notch ECD is also modified with *N*-linked glycans (Fig. 1), which are usually found in contexts outside of EGF-like repeats, but consensus sequences for these types of glycans can be found on some EGF-like repeats on Notch ECD. The Notch ECD has four known sites of *N*-linked glycan modification (Fig. 1) (Haltiwanger and Lowe 2004). *N*-linked glycans are typically made up of seven or more monosaccharaides - the nature of the linkage within a *N*-glycan varies by processes and functions on a glycoprotein (Fig. 4A). Mature *N*-linked glycans

possess a core sequence of sugars that can be classified into 3 main types: oligomannose; complex; and hybrid (Fig. 4B) (Varki, Cummings et al. 2009). They are linked to the amide Nitrogen of an Asn within the consensus sequence N-X-S/T. Synthesis of an *N*-linked glycan initiates with the transfer of a GlcNAc from a donor UDP-GlcNAc to the lipid-like precursor Dolichol phosphate to generate Dolichol pyrophosphate *N*-acetylglucosamine (Fig. 4A). Sugars are sequentially added to Dolichol-phosphate to create a 14-sugar core glycan that is flipped over to the luminal side of the ER while being synthesized (Fig. 4A). This entire glycan is then transferred to proteins containing the N-X-S/T consensus sequence being translocated through the Endoplasmic Reticulum membrane (Fig. 4C). Trimming of the 14-sugar core occurs in the ER with the help of glycosidases (Fig. 4C). The remodeling of the *N*-glycan in the ER plays an important role in folding of many proteins (Helenius and Aebi 2004). After a series of reactions, the properly folded glycoprotein then travels to the Golgi apparatus, where late maturation occurs through the sequential activities of glycosidases and glycosyltransferases to generate the mature *N*-glycan structures (Fig. 4B).

One of the goals of this project required development of robust and rapid methods to analyze *N*-glycan structures. A number of published methods are available, and we decided to test a recent method published by Dr. Nicole Packer's laboratory (Jensen, Karlsson et al. 2012). The *N*-glycan is first released from protein using the enzyme peptide-*N*-glycosidase F (PNGase F). This enzyme is an amidase that cleaves the bond between the asparagine residue on glycoproteins and the innermost GlcNAc (Fig. 5). It works on all types of *N*-glycans including high mannose, complex, and hybrid oligosaccharides (Fig. 4B). Once the *N*-glycan is released, several different methods can be used to analyze the structure of the released glycans (Wada, Azadi et al. 2007). Three primary methods are used currently in the analysis of *N*-linked glycans: fluorescently derivatized glycans separated by LC (Guile, Rudd et al. 1996), permethylated glycans analyzed by matrix-assisted laser desorption/ionization (MALDI)-MS (Kang, Mechref et al. 2005), and glycans separated on a porous graphitized carbon (PGC) and analyzed by LC-MS (Wuhrer, de Boer et al. 2009, Jensen, Karlsson et al. 2012). We chose to use the latter method using a PGC-LC-ESI-MS/MS apparatus. The advantage of using this method is that it does not require any derivatization of the released glycan and we are able to achieve isomer separation, a feature that neither of the other two methods allow us to do. The PGC chip has high resolving power, and is also compatible with a wide range of pH.

There are four EGF-specific *N*-glycan sequons present on the mouse Notch 1 ECD, all of which are predicted to be modified with *N*-glycans (Fig. 1). The sequons are present on EGF-like repeats 23, 25, 30, and 32. Not only are *N*-linked glycans found on Notch, but also on protein modulators of Notch signaling. The primary peptide sequence of Lunatic Fringe suggests a single site for *N*-linked glycan addition. Although there is evidence that these modifications exist, the exact structures have not been identified. One of our goals in this project is to develop methods of glycan release and analysis to identify the exact glycan structure present on Notch ECD and on Lunatic Fringe.

Complex-type *N*-glycans are frequently modified with fucose (Fig. 4B). Since the Fringe enzymes add a GlcNAc to fucose, it is possible that Fringe could modify fucose residues on *N*-glycans. Preliminary data from the Haltiwanger lab suggests that Lunatic fringe modifies itself on its *N*-glycan; however, the results remain inconclusive. The other goal of this project is to examine this self-modification in more detail. Results of this experiment can be combined with structural analysis data on Lfng glycans to gain a better understanding of the structural components and enzymatic specificity of Lfng.

II: Materials and Methods

Materials

- 100 mm cell culture dish
- 15 mL Falcon tubes
- 300 mm (length) x 14 mm (diameter) Sephadex G-50 beads (Pharmacia Fine Chemicals) packed in 1X G-50 buffer (50mM Ammonium formate, 0.1% SDS, 0.02% Sodium azide)
- 96-well plate
- Acetone
- Acetonitrile
- Ammonium acetate
- Ammonium formate
- CHO cells
- Clean razor blade
- Coomassie stain
- Direct Blue 71 (Sigma-Aldrich, catalog no. 212407-50G)
- DMEM
- EN3HANCE
- Ethanol
- Formic acid
- Freezer at -80^{o}C
- Gel drying apparatus
- Glacial acetic acid
- HEK 293T cells
- HEPES
- Hydrochloric acid
- IgG DNA plasmid
- Incubator at 37^{o}C
- Kimtech Science Kimwipes tissues
- Agilent 6330 Ion Trap LC-ESI mass spectrometer
- MAN-9 glycan standard (Sigma-Aldrich, CAS no. 71246-55-4)
- Mass spectrometer sample collection tubes
- MEM
- Methanol
- Micro centrifuge
- Micro centrifuge tubes
- $MnCl_2$
- Mouse Lfng DNA plasmid
- NP-40
- OPTI-MEM

- Para film
- Pasteur pipettes
- PBS (Phosphate Buffered Saline)
- Petri dish
- PGC chip, Agilent
- Pipette aid
- Pipette tips
- PNGase F
- PVDF membrane
- PVP40 (Sigma-Aldrich, catalog no. PVP40-50G)
- Refrigerator at 4^{o}C
- Scintillation counter
- SDS
- SDS-PAGE apparatus
- Sodium azide
- Sonicator
- SpeedVac
- Stock Ovalbumin
- Trypsin
- UDP-[^{3}H]GlcNAc
- Undeveloped X-ray film and development apparatus
- Water
- Western blotting apparatus

Cell splitting and protein purification

Splitting cells in culture. HEK293T or CHO cells were obtained and grown in a 100 mm dish until they reached an estimated 100% confluence. Following this, the cells were split. Media already present on the cells was first aspirated, and 5mL of PBS was gradually added to the dish to remove any media still in the dish. It is important not to agitate cells when they are exposed to PBS, as this will affect our overall protein yield. After gently tilting the dish in different directions, making sure the PBS has made contact with the entire surface, the PBS was aspirated and 1mL of trypsin was added to the dish. Trypsin causes cells to lift from the dish, which allows for all cells to be easily split and moved to multiple plates. These cells were incubated for 5 minutes at 37^{o}C, after which 9 mL of DMEM media was added to the cells. The type of media used varies depending on the type of cells we are working with: for HEK 293T cells, we used

DMEM; for CHO cells, we used alpha-MEM. Both mediums were supplemented with 10% Bovine Calf Serum (BCS). A pipette aid was used to separate the cells, and to make sure all contents of the tray were homogeneous to the naked eye. In a separate tray, 7.5 mL of DMEM (or MEM) was added with 2.5mL of our original cells mixed with fresh media. This constitutes a 1 in 4 split of cells. Split cells in the new tray were placed in a 37^{o}C incubator and the remaining cells from our original tray were lysed with bleach.

Transfecting split cells with DNA plasmid (IgG or mLfng). After 12 to 24 hours of incubation, cells were transfected with the appropriate DNA plasmid. In our experiments, we used plasmid for mouse Lunatic Fringe (Lfng) and the heavy chain for human IgG (IgG). The Lfng plasmid contained a sequence encoding a poly Histidine tag which enables protein purification using Nickel-NTA beads; IgG does not need a poly Histidine tag as it is secreted at much higher quantities and can be purified using protein A beads if needed. In a separate tube, 6 μg of our selected plasmid DNA, obtained from other lab members, was added to 600 μL of OPTI-MEM. OPTI-MEM is a serum-free cell culture media that is used when transfecting cells. To this, 36 μL of polyethylenimine (PEI) was added; PEI condenses DNA into a positively charged particle which can interact with anionic cell surface residues on target cells to allow for easy endocytosis. This mixture was allowed to sit for 10 minutes, and then was added to the un-aspirated cell plate in a drop-wise fashion. After 4 to 6 hours, the plate media was changed from DMEM to OPTI-MEM to facilitate transfection. These cells were grown to an estimated 100% confluence, which usually takes around 3 days of incubation. The media from our cell plate, containing secreted proteins, was then collected.

Purifying protein. As mentioned previously, IgG is expressed at a high level, so protein purification was not necessary. Lfng was further purified from the media using Ni-NTA beads. 100 μL of packed Ni-NTA beads were initially washed with wash buffer (0.5M NaCl and 10mM imidazole). After one wash, the beads were added to our collected media. The tube was incubated at 4^{o}C (cold room) on an end-over-end rotator overnight. The next day, the tubes were spun for 5 minutes at 3000 RPM so all beads would collect at the base of the tube. The supernatant was removed and the beads were washed twice with wash buffer, using ten times the original packed beads volume. Each time, the beads were spun at 3000 RPM for 5 minutes to allow the beads to settle, and the buffer would be aspirated. Theoretically, the beads, through an interaction between the poly Histidine tag imidazole groups and the Ni-NTA beads, will have

captured all of our Lfng protein. All non-specific interaction with the beads will be competed off by the 10mM imidazole in wash buffer. To elute our protein, we added elution buffer (250mM imidazole) at twice the volume of packed beads. The high concentration of imidazole will compete off His-tagged proteins from the beads and we would be able to collect our target protein in the supernatant. Beads were washed twice with elution buffer, and supernatants were pooled.

Preparing Ovalbumin. Stock Ovalbumin was added to PBS in appropriate amounts to prepare necessary concentrations of protein.

Glycomics protocol using PVDF membrane (based on Jensen et al. 2012)

Dot-blotting on to PVDF membrane. A piece of membrane was cut and activated through wetting in 100% ethanol and then placed on top of an ethanol-wetted tissue. Protein solution of at least 2 μg / μL was spotted with approximately 1cm distance between the spots. The membrane was left to air-dry at room temperature to ensure that all protein was fully bound to the membrane.

Staining PVDF membrane. The protein-bound membrane was washed twice with 100% methanol by shaking in a Petri dish for 15 minutes. Salts were removed from the membrane by washing in H_2O for 15 minutes. Direct Blue wash solution (20 ml, 40% ethanol; 10% acetic acid) and 1.6ml of Direct Blue 71 stock solution (0.1% wt./vol. Direct Blue 71 in dH_2O) was mixed and used to stain the membrane until distinct spots appeared. Once the spots were clearly visible, the membrane was destained in wash solution followed by a wash in H_2O to remove any acids. The membrane was left to air-dry overnight.

Deglycosylating glycoproteins on PVDF membrane. The protein spots were carefully cut out of the membrane with a razor blade. Each spot was placed in a separate well in a 96-well plate, with the protein side facing up. Before placement of spots in the wells, each well was filled with Polyvinylpyrrolidone (PVP40) solution (1% wt./vol. PVP40 in 50% vol./vol. methanol). PVP40 binds to the PVDF membrane at areas where there is no protein bound, thereby preventing any nonspecific molecules binding to the membrane. The plate was shaken for 5 minutes and the

PVP40 solution was then removed. After three washes with water, each for 5 minutes, all liquid from the wells was aspirated and 5 mL of PNGase F (0.5 U/mL) was added to each well. The 96-well plate was incubated in 37^{o}C for 15 minutes. Water (10 mL) was added to each well, and the plate was incubated overnight.

Collecting sample for mass spectrometer analysis. After incubation, the plate was sonicated in a bath sonicator for 5 minutes, and samples from each well were collected in individual tubes. The wells were washed twice with 20 μL of H_2O and washes were pooled with sample. 10 μL of 100 mM ammonium acetate (pH 5) was added to the samples in order to remove glycosamines from the reducing terminus of PNGase F released glycans. The samples were incubated at room temperature for 1 hour. Samples were dried in a SpeedVac concentrator without heating and stored in -20^{o}C until analyzed by PGC-LC-ESI-MS/MS.

Analyzing using Porous Graphitized Carbon LC-ESI MS. Before injection in the mass spectrometer, our purified glycan samples were re-suspended in 97% Buffer A (0.1% formic acid in H_2O) and 3% Buffer B (95% acetonitrile and 0.1% formic acid in H_2O) for a final volume of 10 μL. Any glycan standards used were initially suspended in 100% H_2O and diluted to the desired concentration with 3% B. 1 μL samples were placed in autosampler vials and inserted into the autosampler. Samples were automatically injected and the following gradient on the nanopump was used at 0.45 μL per minute flow rate:

Times	Buffer A (0.1% formic acid)	Buffer B (95% acetonitrile, 0.1% formic acid)
0 minutes	95%	5%
15 minutes	50%	50%
20 minutes	5%	95%
25 minutes	5%	95%
26 minutes	95%	5%

The capillary voltage for the mass spectrometer was set to approximately 1750 Volts, achieving a current of approximately 60 nano Amps. These values were optimized for each run to ensure an appropriate “J-shaped stream”. The ion trap settings were optimized for each run based in the

'Optimize' tool, which used the data gathered from a preliminary standard run. Dry gas flow was at 5 liters per minute and temperature was set at 325^{o}C. Interpretation of data was done manually through analysis of chromatograms generated through our apparatus. For every chromatogram, a BPC (base peak chromatogram) was generated; a BPC represents intensities of the most abundant ion in each scan eluted at different times through our PGC chip. Intensities of peaks are directly proportional to concentrations of the corresponding molecules eluted at a specific time point. Within the BPC, the contents represented by each peak can be further analyzed through fragmentation data generated for select molecules that are eluted at a certain time point; this is known as an MS/MS. For glycans that did not show significant peaks in the BPC, EICs (extracted ion chromatograms) were generated by searching for ions with a mass-to-charge ratios (m/z) corresponding to a specific glycan (e.g. $Man_9GlcNAc_2$ glycan standard and *N*-glycans on IgG). An EIC is the representation of only the ion with the specific m/z as it elutes during an entire chromatographic run. Once an ion with the appropriate m/z has been identified (called a parent ions), their identity can be confirmed by Collision-induced dissociation (CID). CID is a process of fragmenting ions by colliding them with helium. We call the spectrum generated from a CID fragmentation an MS/MS spectrum. Glycans fragment mainly at glycosidic bonds, so the daughter ions show differences in masses corresponding to the masses of monosaccharides: 162.14 for hexoses (Glc/Man), 203.19 for HexNAc (GlcNAc), and 146.14 for deoxyhexoses (Fuc). Note that we cannot tell the difference between hexoses (Glc/Man) based on mass alone. For unknown glycans, neutral monosaccharide loss searches were used to match MS/MS patterns corresponding to possible glycans based on the loss of MS monosaccharide masses. Once a possible glycan chromatogram was identified, the known *N*-linked glycan biosynthetic pathway was used to determine branching sequences (Fig. 4A).

Modified glycomics protocol with Western blotting

Western-blotting on PVDF membrane. Glycoprotein was separated by SDS-PAGE and blotted on to a PVDF membrane using a standard Western-blotting protocol. The glycoprotein band was visualized on the PVDF membrane after staining with Direct Blue 71 using the above-mentioned

protocol. This method was used to create a purer sample of *N*-glycans specific to our glycoprotein of choice.

Lunatic Fringe self-modification assay

Preparing reactions/control mixtures for self-modification. In the self-modification experiment, two things are being tested: whether Lfng can modify itself by enzymatically incorporating [^{3}H]GlcNAc on itself, and whether this incorporation is in fact on the *N*-linked glycans of Lfng. mN1 EGF 1-5 has three known O-fucose sites and is known to be modified by Lfng with the addition of a GlcNAc on some of the fucoses (Al-Shareffi, Chaubard et al. 2013). Therefore, EGF 1-5 was used as a positive control for Lfng activity. Since EGF 1-5 does not have *N*-linked glycans attached to it, PNGase F digestion would not cause a diminished radioactive signal after [^{3}H]GlcNAc incorporation. Thus, EGF 1-5 was also used a negative control for PNGase F activity. Ovalbumin is modified by one *N*-linked glycan and served as our positive control for PNGase F catalyzed *N*-linked glycan release. Reaction mixtures for these three conditions (Lfng, Ovalbumin, and EGF1-5) were prepared. In the EGF 1-5 reaction mixture, 10 µg of Lfng from HEK293T cells was added to 10 µg of EGF 1-5. 1uCi of UDP-[^{3}H]GlcNAc, 10 µL of 10X buffer and H_2O were mixed to create a final volume of 100 µL. The buffer consisted of 50 mM HEPES and 10mM $MnCl_2$ with a pH of 6.8. For the Lfng reaction mixture, the same ingredients were used without the addition of EGF1-5, for a final volume of 100 µL. 10 µg of Ovalbumin was added in the final mixture with the same amounts of UDP-[^{3}H]GlcNAc and 10X buffer for a final volume of 100 µL. The labeling reaction mixtures were sealed and incubated in 37^{o}C overnight.

Releasing *N*-linked glycans using PNGase F. Following the overnight incubation, Buffer A (5% beta-mercaptoethanol and 5% SDS) with a final concentration of 1% SDS was added to each sample. The samples were heated for 5 minutes and centrifuged as 14,000rpm for 1 minute. Buffer B (0.7% NP-40 and 50mM tris-HCL at pH 8.0) was added to each of the samples. The three reaction mixtures were then split into PNGase F treated and untreated groups with the addition of 5 µL PNGase F (5U/ µL) to the appropriate tubes. All samples were incubated overnight at room temperature.

Size-exclusion chromatography, scintillation, lyophilization and acetone precipitation. Size exclusion chromatography was performed on all samples using G-50 buffer (50mM ammonium formate; 0.1% SDS; 0.02% sodium azide) as the eluent on a Sephadex G-50 bead column. 30 eluted fractions (1 ml) were collected for each sample, and aliquots from each fraction were tested for radioactivity using a scintillation counter. Fractions that were suspected to contain protein (void volume), as suggested by positive radioactivity counts in the EGF 1-5 collections, were pooled and lyophilized overnight. Acetone precipitation was performed by the addition of about 8mL of cooled acetone to tubes contained our sample proteins. These samples were incubated at -4^{o}C overnight to allow precipitation of protein to occur, after which all acetone was aspirated from tubes.

Performing SDS-PAGE and autoradiography. Each sample was resuspended in 20 μL of SDS-sample buffer and separated by SDS-PAGE and stained with Coomassie. The appearance of appropriate protein bands under each lane suggested the successful activity of PNGase F and protein purification. The gel was activated using the scintillator EN^{3}HANCE and then dried. The dried gel was sandwiched against a sensitive X-ray film, and exposed in -80^{o}C. The film was developed after 2 months of exposure, and results compared with the original dried gel containing protein.

III: Results

Analyzing a $Man_9GlcNAc_2$ standard using the HPLC Glycan CHIP-MS/MS

In order to test the effectiveness of our *N*-linked glycan structural analysis protocol, individual steps of the protocol were tested for effectiveness. We first tested our HPLC chip coupled MS apparatus with a known glycan standard. For our protocol, the HPLC chip contained porous graphitized carbon (PGC). A stock solution of 1 μg /ml $Man_9GlcNAc_2$ (MAN-9) standard was injected and the resulting spectra was analyzed. MAN-9 has a molecular weight of 1883.67 therefore an m/z ion around 942.8 would suggest MAN-9 ion present in the +2 charge state (Fig. 7A). A BPC with two prominent peaks was observed (Fig. 7B). A parent ion of mass-to-charge ratio 942.8 was observed under the first prominent BPC peak (Fig. 7C). MS/MS data for this ion produced a fragmentation pattern that is consistent with the injected glycan standard (Fig. 7D). A second BPC peak that was observed, at a later elution, also contained a parent ion with an m/z value of 942.9 (Fig. 7E). Fragmentation of this peak also produced the previously observed MAN-9 glycan standard fragmentation pattern (Fig. 7F). These results suggest that both peaks in the BPC correspond to the same glycan molecule but at varying elution times. The two peaks arise due to anomerization of carbon at the reducing end of the released glycans.

The presented results correspond to the injection of 530 femtomoles of MAN-9 glycan standard. Injection of MAN-9 standard at varying concentrations was done, and similar results were obtained. The count intensity for glycan standard molecules was affected in a dose-dependent manner. The lowest amount of MAN-9 glycan used was 5.3 femtomoles and it was found to be detectable on our apparatus at this concentration.

This result demonstrated that the PGC chip worked in our hands. Glycans present in our sample could be successfully analyzed using our mass spectrometry apparatus. The next step would be to grow cells expressing protein with known *N*-linked glycans, isolate and purify glycans from this protein, and use the mass spectrometer to analyze collected *N*-linked glycan structures.

Analyzing N-linked glycans from Immunoglobulin G using the glycomics protocol

In order to test the deglycosylation and analysis protocol (Fig. 6), we used a well-characterized glycoprotein. IgG has one known *N*-linked glycans and the structure of the glycan is well characterized (Fig. 8A) (Rademacher, Homans et al. 1986). Purified N-linked glycan on our sample of IgG protein was injected through our MS apparatus and a BPC was generated (Fig. 8B). The IgG *N*-linked glycan has a mass-to-charge ratio of 1462. Several prominent peaks were observed in an extracted ion chromatogram (EIC) for a mass-to-charge ratio of 732 (Fig. 8C). This value corresponds to the IgG glycan ion in a +2 charge state. As our glycans were not reduced before injection into the PGC chip, we expected to see two prominent peaks suggestive of our glycan's alpha and beta anomers. Interestingly, in the 732 m/z EIC we observed two large peaks and a single division in each large peak, creating four total peaks. A parent ion of m/z 732.8 was observed at the larger of the earlier elution peaks (Fig. 8D). After MS/MS fragmentation analysis, this ion was found to match the IgG glycan molecule (Fig. 8E). Similar results were obtained for the latest elution peak (Fig. 8F-G). All major peaks were analyzed and the IgG glycan was observed in all four. The splitting larger peaks into two peaks eluting at different times was credited to our mass spectrometer apparatus- this effect was observed only in IgG glycan analysis. These results proved that our methods of protein and subsequent glycan purification were effective.

Analyzing the N-linked glycan modification on Lunatic Fringe using the glycomics protocol

Having verified all steps of our protocol, these same methods were then used to analyze the structures of *N*-linked glycans on Lfng produced in Lec1 Chinese Hamster Ovary (CHO) cells. Two major peaks were observed in the BPC for our purified Lfng glycan sample (Figure 9A). MS/MS fragmentation was performed on the parent ions from these peaks and a possible glycan structure was discovered with mass-to-charge ratio of m/z 1235.9 in the +1 charge state (Figure 9B-C). The preliminary structure for this glycan suggests a core *N*-inked glycan with 2 GlcNAcs followed by branching of 5 Mannoses (Figure 9F). The BPC for our purified glycan shows two peaks that occur at varying elution times: a smaller peak that elutes around 5.6 minutes and a larger peak that elutes at 6.2 minutes. As seen in our previous glycan runs, we

believed these peaks belonged to the same glycan molecule. The glycan structure mentioned previously was from the earlier elution. A parent ion obtained from the later elution peak was identified, with a m/z value of 1236.0 (Fig. 9D). Fragmentation of this parent ion showed that this parent ion was the same as the glycan that was eluted earlier (Fig. 9E).

Although the fragmentation pattern did not suggest the presence of a fucose on this structure, an EIC of our glycan mass with the exact addition of one fucose revealed two major peaks (Figure 9G). The peak observed in an EIC at 1381 m/z for our sample did not have MS/MS fragmentation data because our apparatus did not select this ion for fragmentation. Furthermore, the intensity of this peak is tenfold less than that for the non-fucosylated form of the glycan (compare panels in Figure 9G). Although our analysis of this peak is incomplete, the data suggests that there is a small amount of fucosylated *N*-glycan on Lfng isolated from Lec1 cells. This data suggests that the *N*-glycans on Lfng grown in Lec1 CHO cells are not abundantly modified with fucose. The Lec1 CHO cells used to produce our Lfng samples lack GlcNAcT-1 and thus are unable to produce complex or hybrid *N*-linked glycans (Fig. 4B). Fucose is typically not seen high mannose type *N*-glycans, so theoretically we would see very little of it on the *N*-glycans of Lfng produced in the Lec1 CHO mutant cell lines. Lfng was also produced in HEK293T cells (which have GlcNAcT1) and *N*-linked glycans were purified. We anticipate that the *N*-glycans on Lfng from the HEK293T cells will be modified with fucose. Mass spectrometry analysis of this sample is pending.

Analysis of Lunatic Fringe's ability to modify its own N-linked glycan

Lunatic Fringe acts by modifying fucose with the addition of a GlcNAc monosaccharide. This modification typically occurs on O-fucose on EGF-like repeats (Moloney 2000), but theoretically it could occur on Fuc found on the core GlcNAc of *N*-linked glycans. Since Lfng is modified with an *N*-linked glycan, and there is data suggesting that there is a fucose on this glycan (Figure 9F), theoretically Lfng would be able to modify N-glycans on itself. Preliminary data in the Haltiwanger lab suggests just this, i.e. that Lfng modifies its own *N*-linked glycan.

To examine this in more detail, we carried out a radioactivity assay that would qualitatively show the addition of GlcNAc by Lfng (Fig. 10A). All reactions contained UDP-[^{3}H]GlcNAc as the donor substrate. Three acceptor substrates were used in this experiment: 1) Lfng with an *N*-linked glycan acceptor fucose; 2) ovalbumin as a positive control for PNGase F activity; and EGF 1-5 as a positive control acceptor for UDP-[^{3}H]GlcNAc catalyzed by Lfng and negative control for PNGase F activity. After overnight incubation followed by PNGase digestion, Size exclusion chromatography was performed on each of these samples; collected fractions were tested for radioactivity using a scintillation counter (Fig. 10B). As a positive control for radioactive substrate addition catalyzed by Lfng, the EGF1-5 aliquots showed considerable radioactivity, suggesting incorporation of [^{3}H]GlcNAc. Neither Lfng nor ovalbumin showed any significant amount of radioactivity incorporated.

The next step was to separate the proteins by SDS-PAGE and perform autoradiography to more accurately test whether [^{3}H]GlcNAc was incorporated into Lfng. A Coomassie stained SDS-PAGE gels of these samples revealed that PNGase F activity was successful, causing a shift in protein band observed in the Ovalbumin lanes and the Lfng lanes (Fig. 10C). This result demonstrated that Lfng has an *N*-linked glycan that is cleavable by PNGase F. The shifted Lfng bands were also observed in EGF1-5 lanes as expected since Lfng is also present in that sample. The Coomassie stained gel was dried, activated and incubated with X-ray film between two boards. The sandwich was placed in -80^{o}C for two months. The developed film showed significant [^{3}H]GlcNAc incorporation on EGF 1-5, the positive control for Lfng activity and a small amount of incorporation into Lfng (Fig. 10D-E). Interestingly, PNGase F digestion of Lfng did not diminish [^{3}H]GlcNAc incorporation on Lfng, suggesting incorporation into a glycan other then the N-glycan. There was no detectable incorporation on Ovalbumin, our negative control for Lfng activity.

IV: Discussion

The primary goal of this project was to develop a robust and sensitive method for analyzing N-glycans. Through our methods, we proved that the PVDF glycomics method produced reliable results when purifying and analyzing known and unknown N-glycans. Through our proven glycomics method, we characterized a preliminary structure for the Lfng N-linked glycan, and have data that suggests a possible fucose on this glycan. Theoretically, it is possible that Lfng could add GlcNAc to this fucose modification present on the N-linked glycan, and prior studies in the Haltiwanger laboratory suggested that this may occur. Our results suggest that Lfng does in fact modify itself, but the site of modification is not certain. Our Lfng self-modification assay results suggest that this site of modification is not on the N-glycan.

We carried out several control experiments to test the effectiveness of our PVDF glycomics protocol, beginning with the analysis of a known glycan. The $Man_9GlcNAc_2$ glycan was injected through a Porous Graphitized Carbon (PGC) chip linked to an ESI-MS/MS and the resulting chromatogram was studied (Fig. 7B). Since this was the only sample we injected in the mass spectrometer, we observed two prominent peaks and almost no noise in the resulting BPC. The peak with highest intensity was observed at 10^7(Fig. 7B). We believe that each peak corresponds to the same structure, but in one of two anomeric forms. This is true because $Man_9GlcNAc_2$ was found to be present in equal concentrations within both peaks (Fig. 7C-F). Our standard glycan exists with a mass-to-charge ratio of 1883 when singly ionized and 942 when doubly ionized. Peaks for the doubly charge glycan were found in both of the major BPC peaks, and fragmentation of these further proved that the mass spectrometer was detecting only our standard glycan. This standard glycan run was important because it proved that our PGC chip worked and that it was possible to determine the structure of a possible glycan through fragmentation data produced by our mass spectrometer.

To test the glycan release method, we used IgG as our sample protein. IgG has a well characterized *N*-linked glycan attached to it with a known mass of 1462.53 Daltons (Fig. 8A). The only difference between the two methods we tested was the manner in which Polyvinylidene fluoride (PVDF) membrane was exposed to sample protein (Fig. 6). The hydrophobic PVDF membrane was used because when protein is loaded on this membrane, the peptide backbone of a glycoprotein interacts strongly with the membrane and polar sugar modifications on the protein

are exposed to the environment. Exposed glycans were cleaved through PNGase F, and collected for analysis. In our first method, IgG was directly spotted on the PVDF membrane and then stained with Direct Blue. The region of membrane with our protein would appear as a deep blue spot, which would then be cut out and used in subsequent purification steps. In the modified glycomics method, the sample protein was run on a gel through SDS-PAGE and then transferred on to a PVDF membrane through Western blotting. The PVDF membrane was stained with Direct Blue; deep blue protein bands would appear on the membrane. The protein band corresponding to our protein of choice would be cut out and used. This method would ensure that a very pure sample of our protein was used but likely affected protein yield present on the membrane. All subsequent steps for the deglycosylation and collection were the same for both methods.

Chromatograms produced by each method were analyzed using IgG as our experimental protein. Since there may have been many contaminants present in our sample before injection into the mass spectrometer, the BPC for either method did not produce prominent peaks as it did for the standard glycan previously. An EIC was generated for the doubly charged form of IgG *N*-glycan. The EIC generated from results obtained through the Western PVDF glycomics method did not yield prominent peaks, however four distinct peaks were observed in the EIC generated through the regular PVDF glycomics method (Fig. 8C). The fact that we did not see any peaks through the Western PVDF glycomics method suggests that there is a significant loss in yield. We suspect this is when protein is being transferred to the PVDF membrane or when the sample protein is acetone precipitated before it is loaded on a gel. There may be some glycan that was deglycosylated and purified, but this method cannot be practically used for analysis through ESI-MS/MS. Thus, the PVDF glycomics method was used for all further experiments due to its sensitivity.

Analysis of peaks in the EIC for the regular glycomics method demonstrated that the IgG *N*-glycan is present in all four peaks. Similar to the standard glycan, we believe that the anomeric forms of IgG *N*-glycan are separated by the PGC, and that they appear as distinct peaks. Fragmentation data from molecules in each of these peaks confirmed the presence of IgG *N*-linked glycan (Fig. 8C-F). The peak with highest intensity for IgG *N*-glycan appeared at 10^5, which is two orders of magnitude less than the standard glycan results we obtained previously, but still intense enough to be fragmented by the mass spectrometer. Our analysis of these

chromatograms demonstrated that the regular PVDF glycomics method can be used to purify and characterize *N*-glycans on purified proteins. This method can be used to characterize *N*-linked glycans on almost any protein. We plan to study the *N*-glycans modifications present at four possible sites on the Notch ECD (Fig. 1). The next step in our sequence of experiments for this project was to use these proven methods to characterize the *N*-glycans present on Lunatic Fringe (Lfng).

Lfng produced in Chinese Hamster Ovary cells (CHO cells) were used in this experiment because this was the only stock sample of Lfng we had available at the time. We later realized that the CHO cells were Lec1 mutant cells, which means they have a mutation in GlcNAcT-1. The BPC produced after *N*-glycan purification showed two prominent peaks, similar to those observed in the BPC of the standard glycan previously, with the most intense peak at 10^6 (Fig. 9A). The fact that we can observe two distinct peaks on the BPC and not just on an EIC, as was the case in our IgG experiment, suggests that our purification methods were effective but only if these peaks correspond to glycan molecules. A neutral loss search for the loss of mannose monosaccharides (168 Da) resulted in the discovery of an MS/MS fragmentation pattern suggestive of a possible glycan structure (Fig. 9B-C). The parent peak of this glycan had a mass-to-charge ratio of 1235.9, was eluted at 5.6 minutes, and has a possible structure of $Man_5GlcNAc_2$ (Fig. 9F). An EIC for this mass-to-charge ratio showed that the same glycan molecule was present in a later elution, around 6.2 minutes (Fig. 9D-E). This suggests that the two prominent peaks observed in the original BPC correspond to the same glycan molecule but in possibly different anomeric forms. Through this method, a preliminary structure for the non-fucosylated *N*-linked glycan attached to Lfng was determined.

Deglycosylation of Lfng from Lec1 mutant CHO cells and subsequent mass spectrometry data suggests that there is a $Man_5GlcNAc_2$ structure present on Lfng. The EIC for non-fucosylated glycan (m/z of 1236) showed peaks for predicted alpha and beta anomeric forms of Lfng *N*-glycan with intensities that are approximately two orders of magnitude higher than peaks produced by the EIC for fucosylated Lfng *N*-glycan (m/z of 1381) (Fig. 9G). Our apparatus did not fragment the putative fucosylated form, which has an intensity that is only a few orders of magnitude away from being interpreted as ‘noise’ by the mass spectrometer. Although it can be assumed through the difference in masses and comparison of EICs that there is a fucose attached

to our Lfng *N*-glycan, our data did not conclusively demonstrate that there is in fact a fucose present.

This low concentration of fucosylated *N*-glycan can be explained by the Lec1 mutation present in cells that were used to grow our sample Lfng protein. When *N*-glycans are being synthesized in the cis-Golgi, GlcNAc-T1 adds a GlcNAc onto the nascent glycan chain. This is the rate-limiting step in maturation of the *N*-linked glycan into hybrid or complex *N*-linked glycans. In Lec1 cells, GlcNAc-T1 is missing and only the oligomannose type *N*-glycan can be produced (Fig. 4C). A core fucose modification would normally be added to hybrid or complex-type N-glycans as the glycan matured through the medial and trans Golgi network but not in the case of cells grown in Lec1 mutant cells. In order to obtain a higher concentration of Lfng *N*-glycans with the fucose modification, we purified the *N*-glycan from Lfng grown in HEK293T cells. Purification of the *N*-glycan was performed however the mass spectrometer results are pending. It is predicted that the intensity of fucosylated glycan will be higher in proportion to non-fucosylated glycan in these results.

From data that was gathered in our experiments, it is suggested that Lfng has a fucose present on its *N*-glycan. Preliminary data from the Haltiwanger lab suggests that Lfng modifies itself, possibly on this fucose; however, there is no conclusive data that proves this hypothesis. In order to test this, we carried out a radioactivity assay (Fig. 10A). Lfng was incubated with UDP-[^{3}H]GlcNAc overnight. To determine whether the modification was specific to the *N*-glycan, half of our resulting reaction mixture was subject to PNGase F digestion. Protein was purified through size-exclusion chromatography in each case and radioactivity was measured through use of a scintillation counter. As a positive control for Lfng's enzymatic addition of GlcNAc to an acceptor fucose, we used mN1 EGF 1-5, with and without PNGase F, in separate reaction mixtures. This peptide sequence contains three sites that are fucosylated; each of these sites would present as a substrate for modification with [^{3}H]GlcNAc. Finally, as a positive control for PNGase F enzymatic cleavage of *N*-glycans we incubated Ovalbumin, with and without PNGase F, in separate reaction mixtures. Ovalbumin is modified with an *N*-linked glycan and has no fucosylated sites.

Initial results obtained after scintillation were not conclusive (Fig. 10B). Lfng did not show any significant radioactivity. EGF1-5 was observed to have significant incorporation of

[^{3}H]GlcNAc and Ovalbumin showed trace amounts of radioactivity when not treated with PNGase F. There is no reasonable explanation for why Ovalbumin showed this trace amount of radioactivity, other than contamination. After scintillation counting was carried out on all samples, the protein samples obtained through size-exclusion chromatography were run on a gel and stained with Coomassie (Fig. 10C). PNGase F treatment caused the expected shift in bands for both Lfng and Ovalbumin. EGF 1-5 appeared as a smear as expected, with no shift due to PNGase F activity due to a lack of *N*-glycans. This gel was then subject to autoradiography, a more sensitive test for radioactivity, for two months. The resulting developed film was compared to our original Coomassie stained gel (Fig. 10D-E).

Ovalbumin did not show any signs of radioactivity, with or without PNGase F activity, which is expected. The fact that we did not see a radioactive band in either of the Ovalbumin lanes suggests that the scintillation counter reading we observed previously was due to contamination. EGF 1-5 showed radioactivity in both PNGase F treated and untreated conditions, confirming that Lfng is able to enzymatically modify O-fucose with [^{3}H]GlcNAc. Since Lfng was included in the reaction mixtures with EGF1-5, it also appears in these lanes; however it is only slightly modified by [^{3}H]GlcNAc. It is visible in the PNGase F treated lane because it creates a clear band that overlaps the EGF1-5 radioactive smear. The lack of a signal in the untreated lane may be due to a loss in sample, as suggested by the fainter band in lane 7 relative to lane 8.

The Lfng band observed in the EGF 1-5 PNGase F untreated mixture was of similar intensity after Coomassie staining as the Lfng band observed in the Lfng PNGase F untreated mixture, which means they are approximately the same amount. After autoradiography the Lfng from the EGF 1-5 PNGase F untreated mixture is not visible, which means none of the Lfng was modified in this mixture. On the other hand, Lfng alone when not treated with PNGase F revealed a visible band on the autoradiograph, which means the Lfng in this mixture was self-modified. It is not clear why Lfng is able to selectively modify EGF 1-5 over itself when the concentration of Lfng (enzyme) and UDP-[^{3}H]GlcNAc (donor substrate) is the same in each mixture. A possible explanation is that there are three sites of modification on each molecule of EGF 1-5 while only one site of modification on Lfng, making it possible for Lfng to favorably target EGF1-5 simply through bulk action. In order to better understand this result, we may want to replicate this experiment with varying concentrations of Lfng and EGF 1-5 to understand the

governing enzyme kinetics. Nevertheless, the modification of EGF 1-5 suggests that our positive control for Lfng activity worked.

Both Lfng lanes, with and without PNGase F treatment, revealed visible bands. The PNGase F untreated mixture revealed a visible signal, suggesting that Lfng does, in fact, modify itself with the addition of a [^{3}H]GlcNAc. Interestingly, the autoradiograph results also suggest that [^{3}H]GlcNAc is not being incorporated on the *N*-linked glycan site as was previously suspected, as deglycosylation of *N*-glycan reveals a prominent signal. If fucose-incorporation were on the *N*-glycan, we would not observe a signal after PNGase F cleavage. Our conclusion from this observation is that although Lfng does modify itself with the incorporation of a [^{3}H]GlcNAc, this modification is not on the core fucose of the Lfng *N*-linked glycan.

Lfng is only known to enzymatically modify fucose, suggesting there may be another site on Lfng that has a fucose attachment that is being modified. There are also other types of glycans that contain fucose such as mucin O-glycosylations. However, the only confirmed glycan modification on Lfng is the *N*-linked glycan. The primary sequence of mouse Lunatic Fringe has a loosely related consensus sequence for O-fucose modification (20CLLVLTA28). The confirmed consensus sequence for modification is CXXXXS/TC and it is only seen in the context of EGF-like and TSR repeats. In mLfng, there is a difference of one amino acid. The consensus sequence for O-fucosylation is not absolute, so it is possible that this variation allows for some fucosylations to occur. Although fucosylations outside the context of EGF and TSR repeats have not been seen yet. This is because the Cys residues at either end participate in disulfide bond formations. Di-sulfide bonds participate in protein folding and they guide the three-dimensional protein structure to form. Without this three-dimensional structure Lfng may be unable to target a possible consensus site, even without a variation in consensus. There is no proof that this may be the site of Lfng modification, but in theory, it would explain our retention of radioactive signal after *N*-glycan loss on Lfng modified with [^{3}H]GlcNAc. A possible future experiment would be to confirm O-fucose monosaccharide modification on mLfng using glycomics and if there is a modification here, we can perform the Lfng radioactivity assay using a fucosidase to cleave possible O-fucose attachments. Another experiment would be to overexpress mLfng in a cell, and look for possible fucosylations through proteomics. Further glycomics and structural analysis must be done to identify the site of Lfng self-modification.

V: Figures

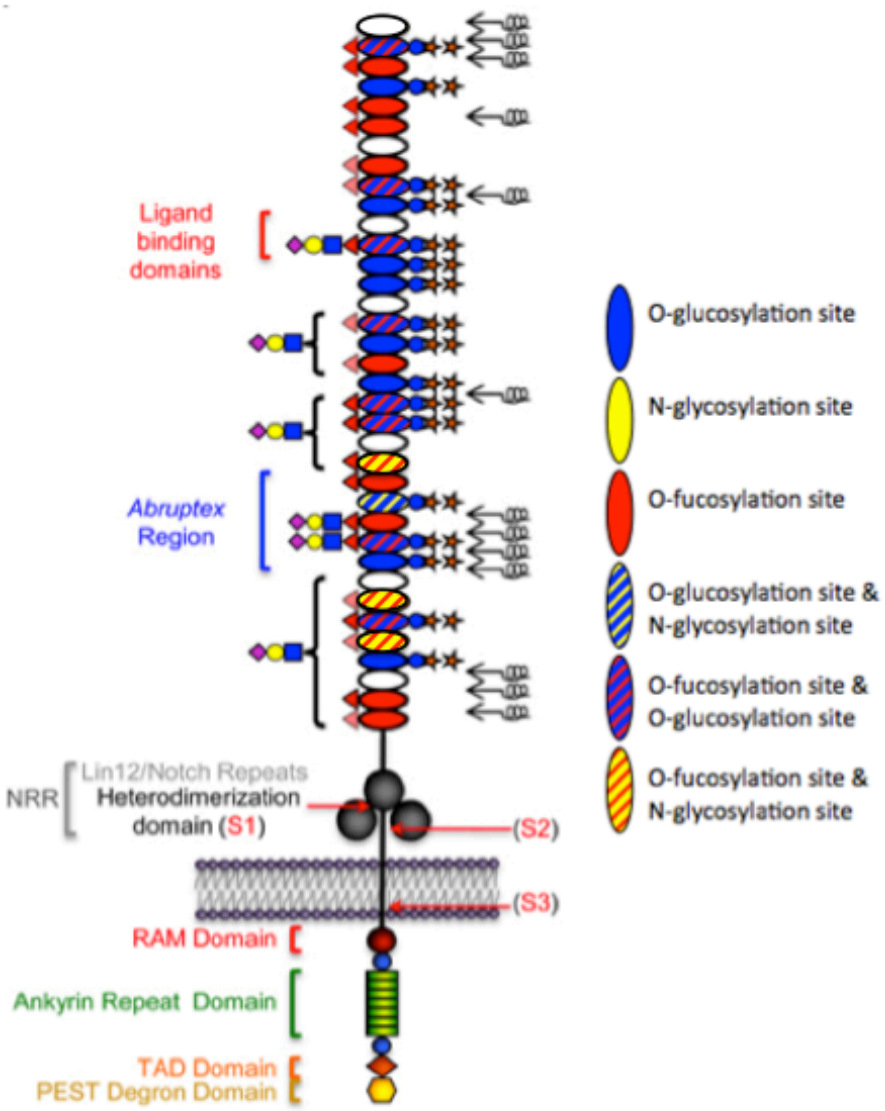

Figure 1: Schematic representation of the extra-cellular domain of mouse Notch 1. mN1 consists of 36 tandem EGF-like repeats (ovals) followed by 3 LIN12/Notch repeats (large gray circles) and a hetero-dimerization domain (black line). EGF repeats consisting of the consensus sequences for any variety of *N*-glycosylation, O-glucosylation, and O-fucosylation have been illustrated in yellow, blue or red respectively. Some sites possess multiple consensus sequences- these are the striped ovals. Symbols are based on Consortium for Functional Glycomics guidelines: glucose, blue circle; xylose, orange star; fucose, red triangle; GlcNAc, blue square; Galactose, yellow circle; sialic acid, purple diamond. Taken from Rana and Haltiwanger (2011).

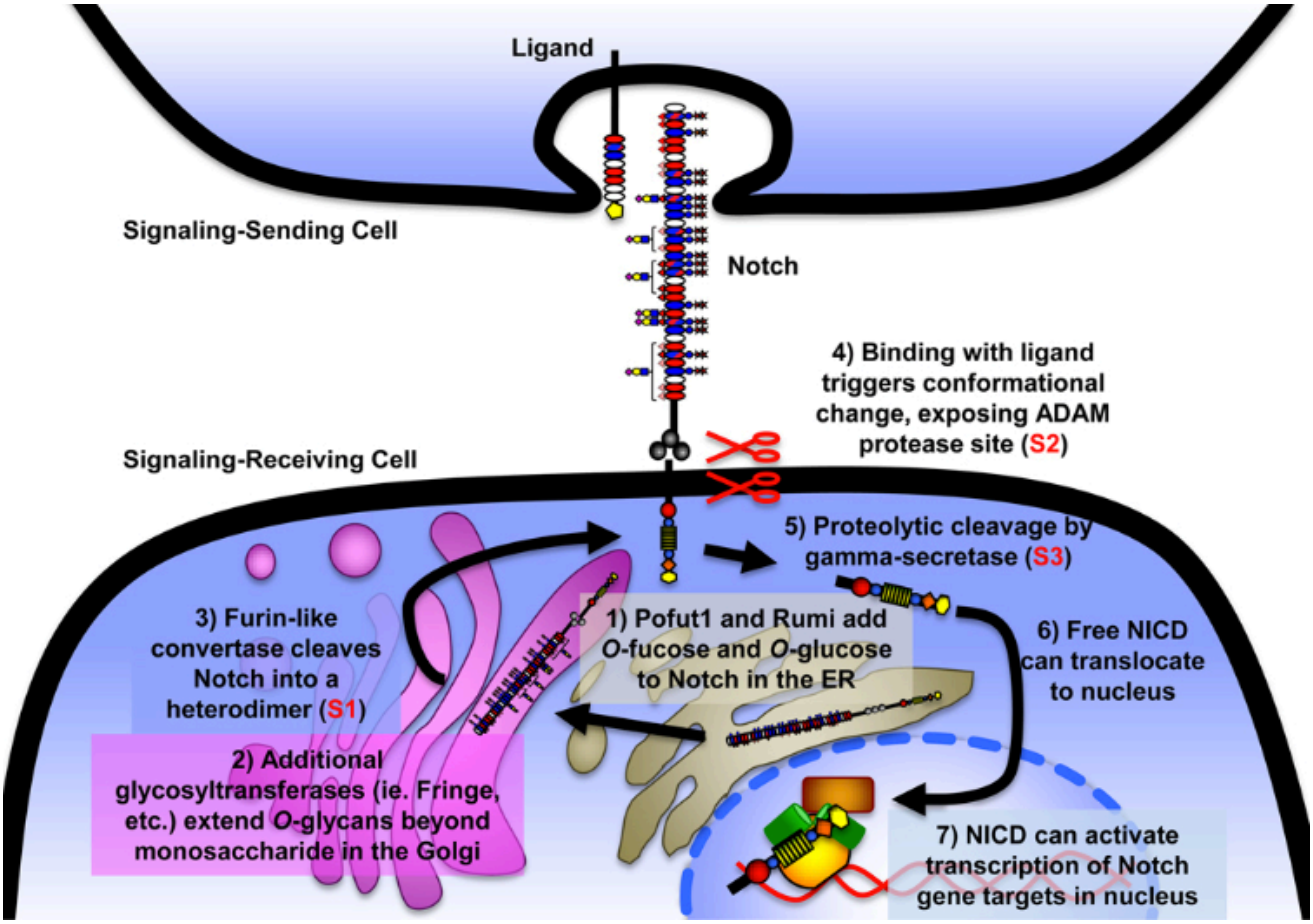

Figure 2: Notch activation pathway. O-fucosylation and O-glucosylation on Notch occurs in the ER (1) and elongation of these initial monosaccharide additions occur in the Golgi by glycosyltransferases (2). In the Golgi, furin-like convertase cleaves Notch at the S1 cleavage site to make a heterodimer (3), which then travels to the surface of the cell where it binds with a DSL ligand. Upon binding, a conformational change exposes the S2 cleavage site, which is cleaved by ADAM protease (4). Proteolytic cleavage of Notch at the S3 site then occurs by gamma-secretase (5) releasing the ICD to travel to the nucleus (6) where it modulates transcription of target genes (7). Taken from Rana and Haltiwanger (2011).

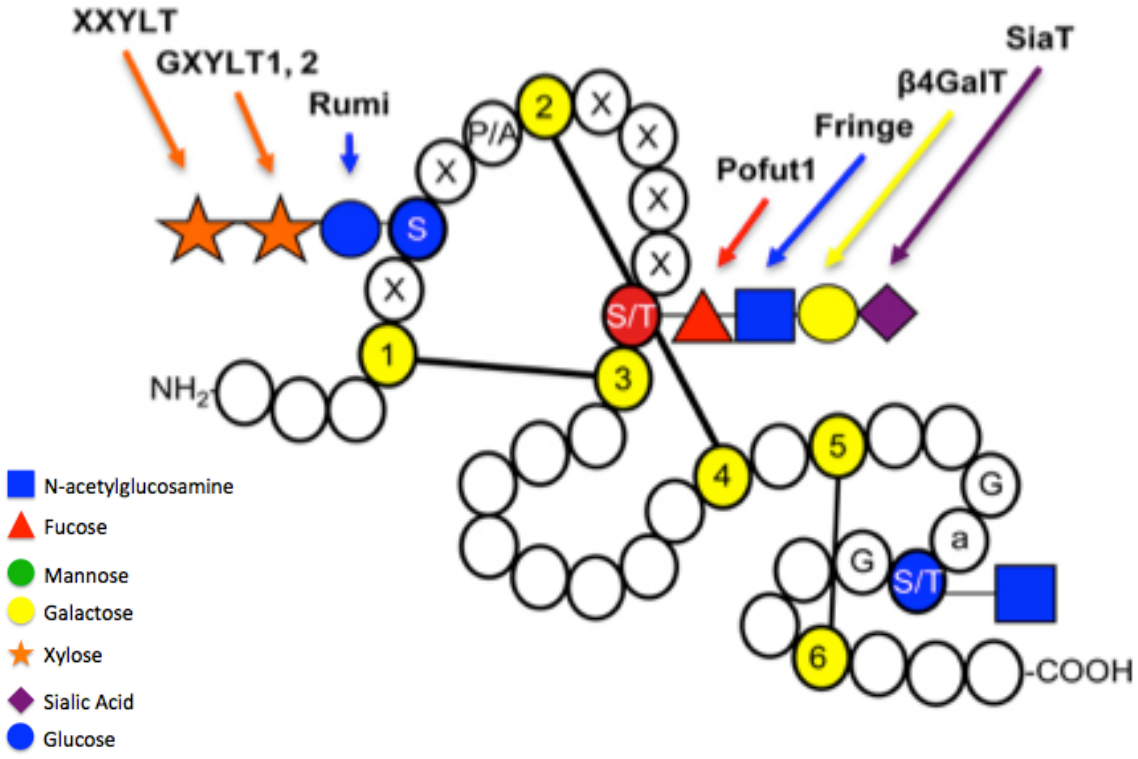

Figure 3: Epidermal growth factor-like repeat found on mN1. The EGF-like repeat is defined by the presence of six conserved cysteine residues that form three disulfide bridges, resulting in a uniquely folded structure. Potential sites of O-glucosylation, O-glucosylation, and O-GlcNAc modification are indicated in blue and red. Arrows indicate Glycosyltransferases that catalyze the addition of sugars. Symbols are based on Consortium for Functional Glycomics guidelines: glucose, blue circle; xylose, orange star; fucose, red triangle; GlcNAc, blue square; Galactose, yellow circle; sialic acid, purple diamond. Taken from Rana and Haltiwanger (2011).

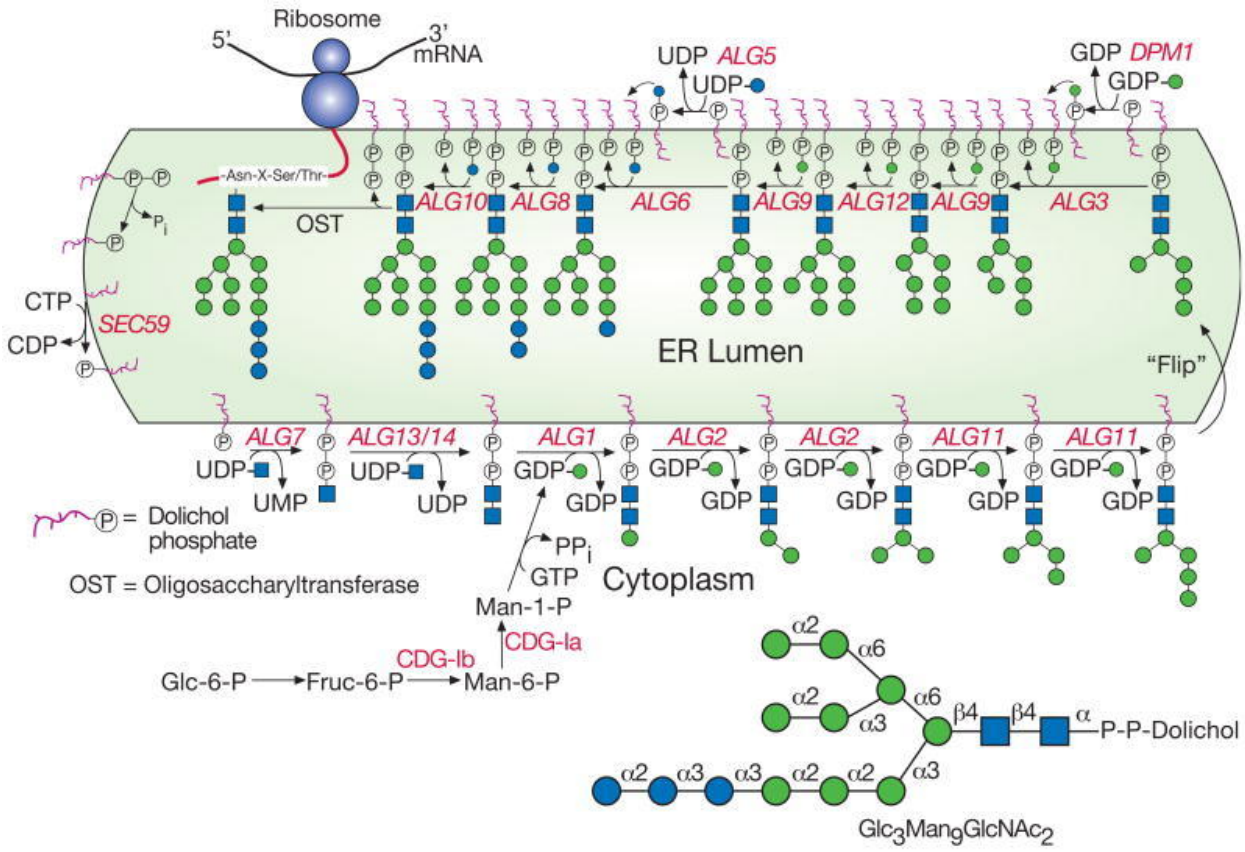

Figure 4A: Biosynthesis of *N*-linked glycan core through modification of Dolichol-phosphate. On the cytoplasmic side of the ER membrane, Dolichol-P is first modified with the addition of GlcNAc from UDP- **[^{3}H]**GlcNAc . Subsequent extensions and branching generates Dol-P-P-$GlcNAc_2$-Man_5, which is then flipped over to the luminal side of the ER. Glucose and mannose resides are added to this oligosaccharide and eventually the entire glycan gets transferred on to the target peptide sequence of the recipient protein. This figure was taken from the *Essentials of Glycobiology* textbook.

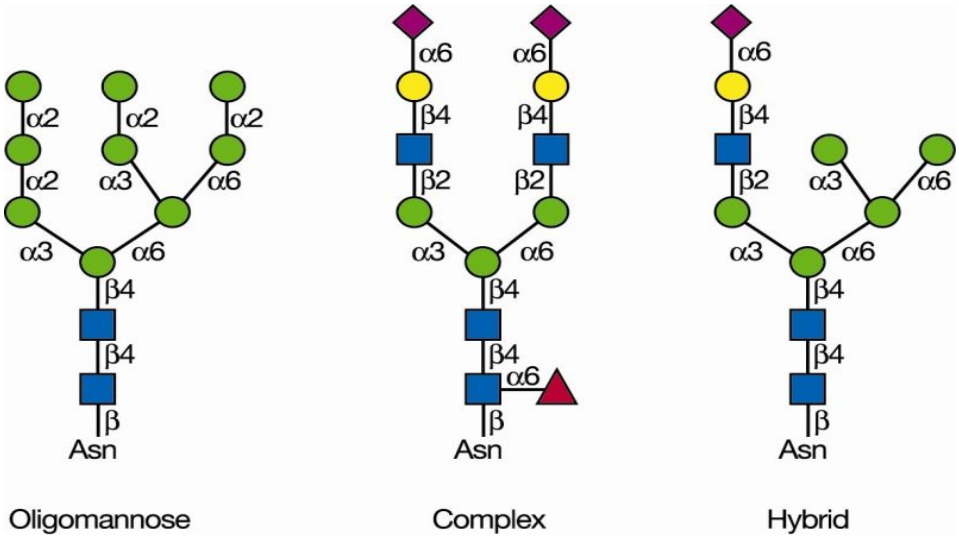

Figure 4B: Common types of *N*-linked glycans. The Oligomannose, complex or hybrid glycans are added to proteins on an Asparagine residue within the Asn-X-Ser/Thr sequon. *N*-linked glycans all have the same core structure: $Man_3GlcNAc_2Asn$. This figure was taken from the *Essentials of Glycobiology* textbook.

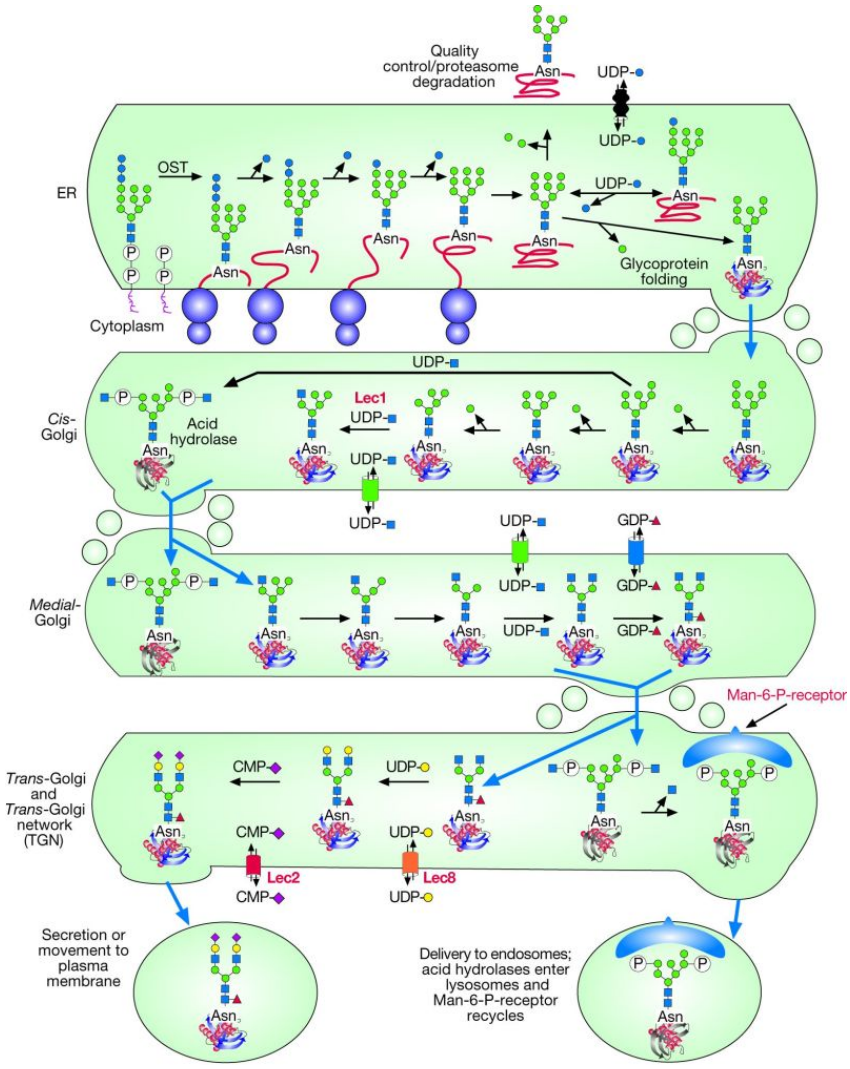

Figure 4C: Maturation of *N*-linked glycans. The Dol-P-P glycan is transferred onto an Asn-X-Ser/Thr sequon. This step is followed by glucosidases removing three glucose residues and mannosidases removing a single mannose from the glycan. The immature glycoprotein is folded in the ER assisted by the lectin-chaperones calnexin and calreticulin. The glycan is subject to further maturation as it moves from the different compartments of the Golgi. In the cis-compartment, mutation in the GlcNAcT-1 enzyme generates a Lec1 CHO type cell line. In these cells $Man_5GlcNAc_2Asn$ is the mature glycan and is not further processed. Further modifications occur until the glycoprotein is either secreted or delivered to the plasma membrane. The image was adapted from the essentials of glycobiology. This figure was taken from the *Essentials of Glycobiology* textbook.

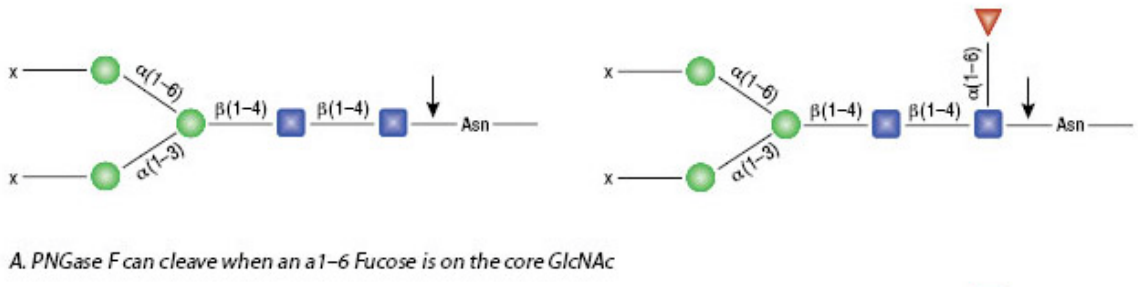

A. PNGase F can cleave when an a1–6 Fucose is on the core GlcNAc

Figure 5: Peptide-*N*-Glycosidase F (PNGase F) cleavage sites. PNGase F is an amidase that cleaves *N*-linked glycans at between the Asparagine residue and innermost GlcNAc. PNGase F is able to do this in oligomannose, hybrid, and complex oligosaccharide modifications on *N*-linked glycoproteins. PNGase F is unable to cleave *N*-linked glycans with a core alpha1-3 fucose attachment. This figure was taken from https://www.neb.com/products/p0704-pngase-f.

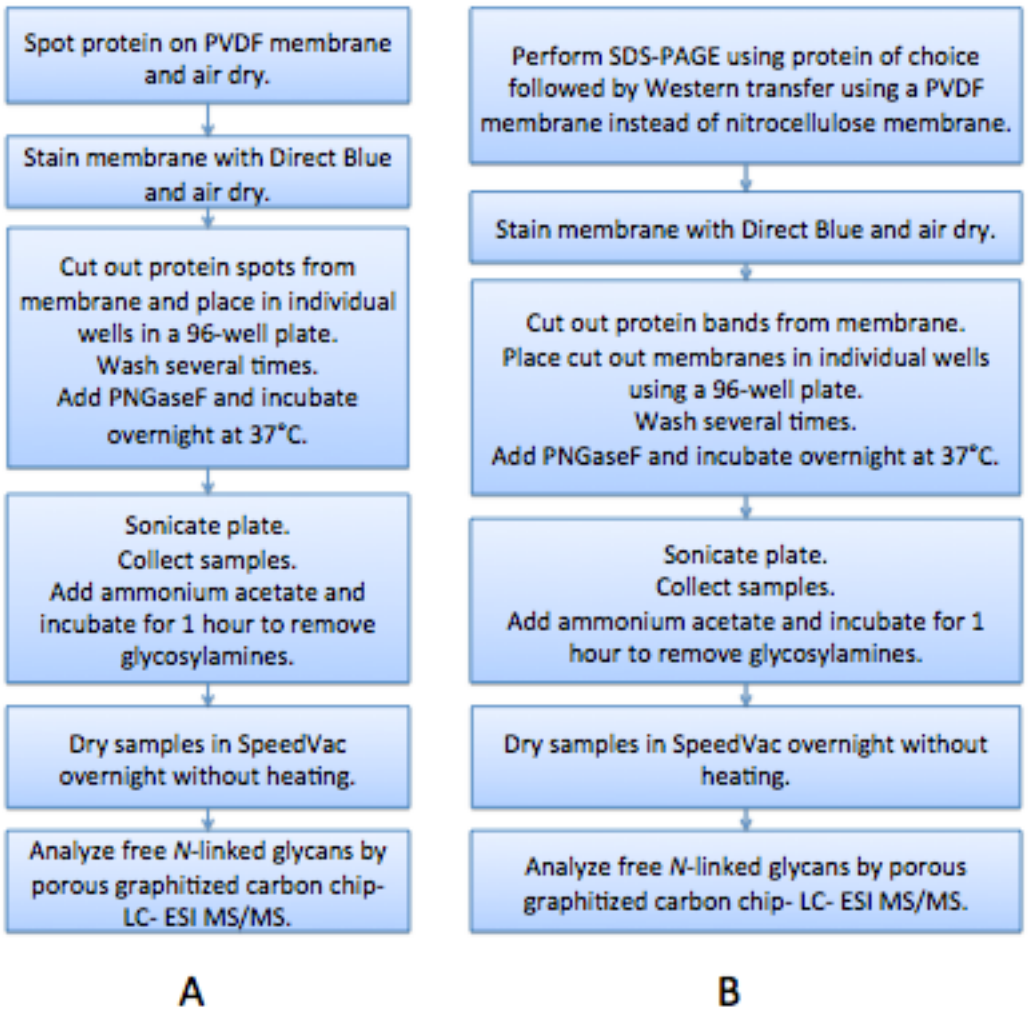

Figure 6: Flowchart of PVDF glycomics method (A) and of Western PVDF glycomics method (B). The only difference between these two methods is how protein was added on to the PVDF membrane. In method A, protein was directly spotted on to the PVDF membrane, while in method B protein was transferred on to PVDF membrane through Western blotting.

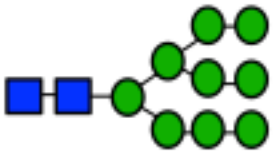

Figure 7A: Structure of pure $Man_9GlcNAc_2$ standard glycan used to test effectiveness of PGC chip linked LC/MS apparatus. The molecular weight of this glycan is 1883.67 Daltons.

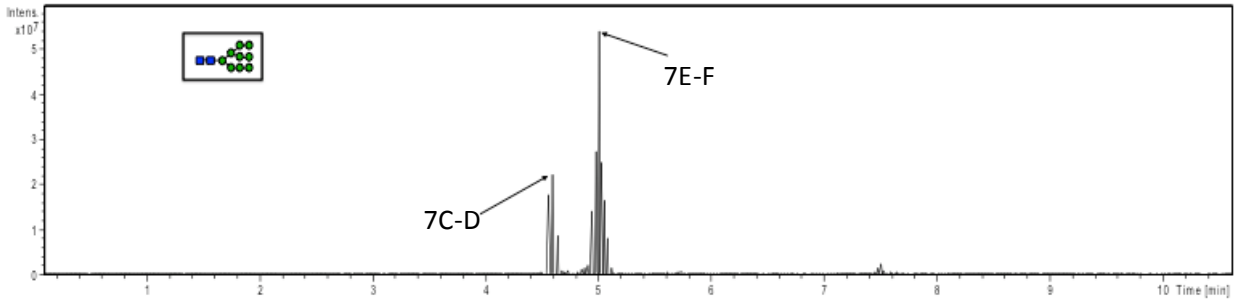

Figure 7B: Base peak chromatogram (BPC) of $Man_9GlcNAc_2$ standard glycan produced from 530 femtomoles of sample.

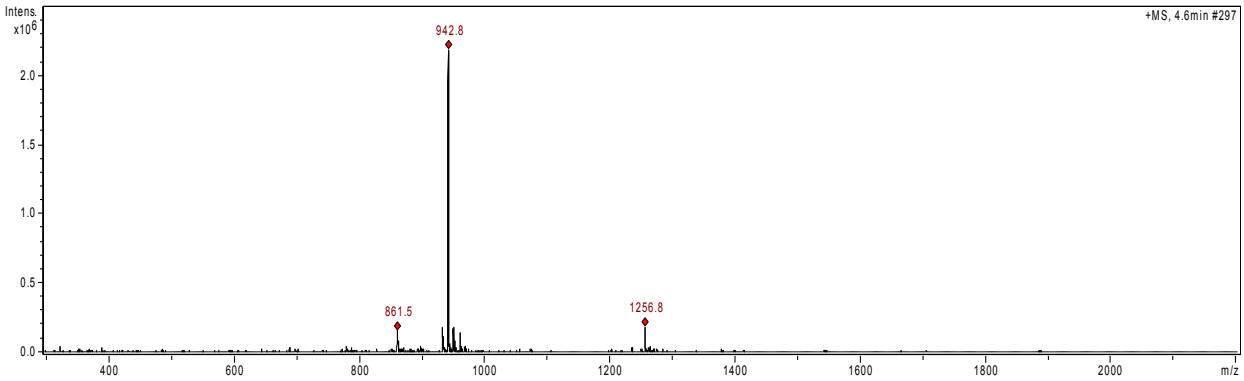

Figure 7C: MS of parent peak with a mass-to-charge ratio of 942.8, observed at approximately 4.6 minutes. This peak corresponds to the glycan standard in a +2 charge state.

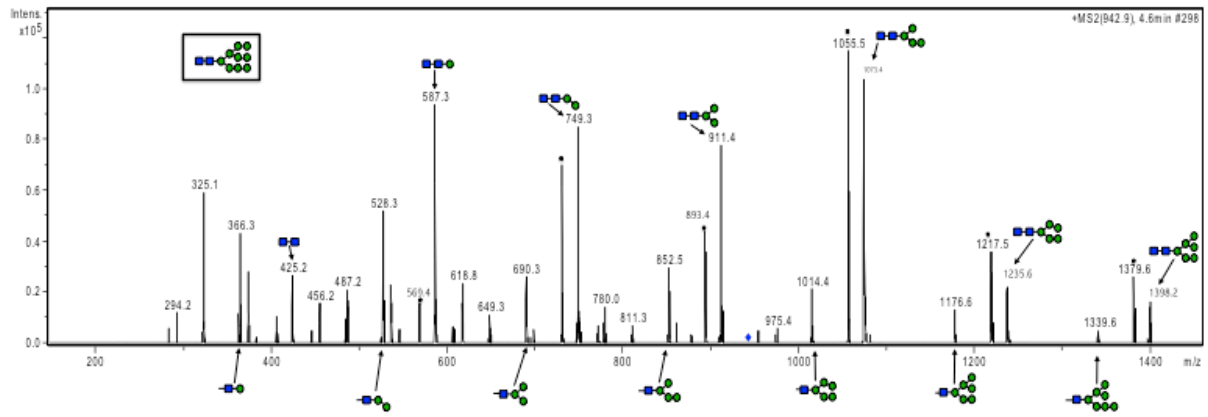

Figure 7D: MS/MS fragmentation pattern of parent peak with mass-to-charge ratio of 942.8 observed at approximately 4.6 minutes. This pattern is evidence that the fragmentation occurred as expected, and the full glycan structure can be determined through analysis of MS/MS data from our apparatus.

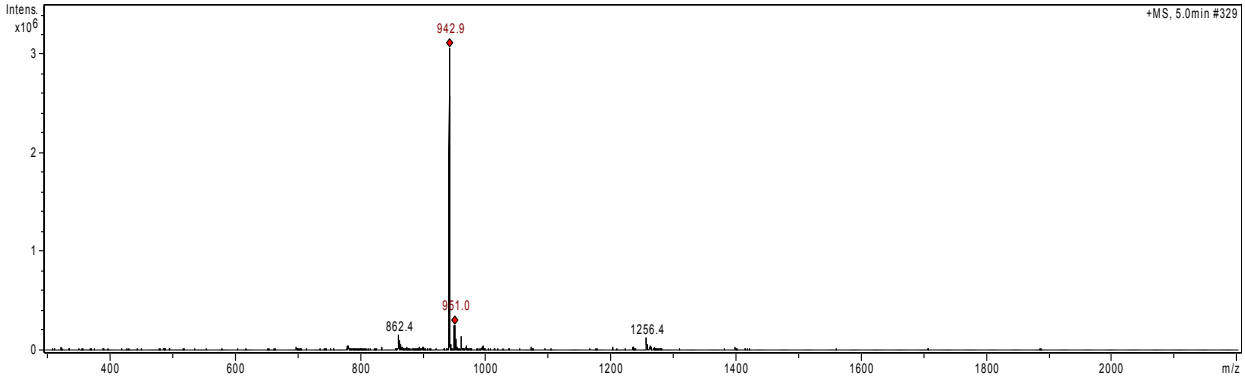

Figure 7E: MS of parent peak with a mass-to-charge ratio of 942.9, observed at approximately 5.0 minutes. This peak also corresponds to the glycan standard in the +2 charge state.

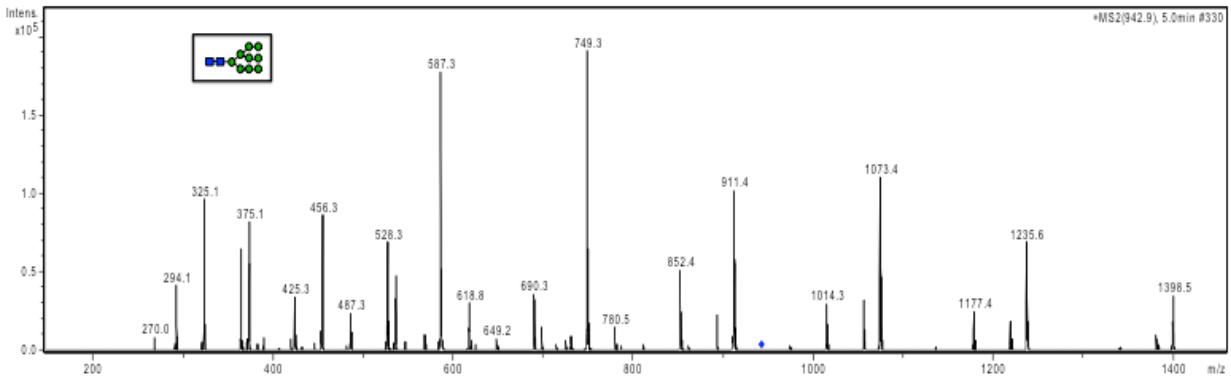

Figure 7F: MS/MS fragmentation pattern of parent peak with mass-to-charge ratio of 942.9 observed at approximately 5.0 minutes. This pattern is evidence that the fragmentation occurred as expected, and the full glycan structure can be determined through analysis of MS/MS data from our apparatus.

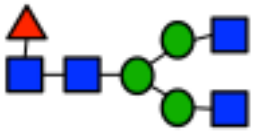

Figure 8A: Known *N*-linked glycan structure has a molecular weight of 1462.53 Daltons.

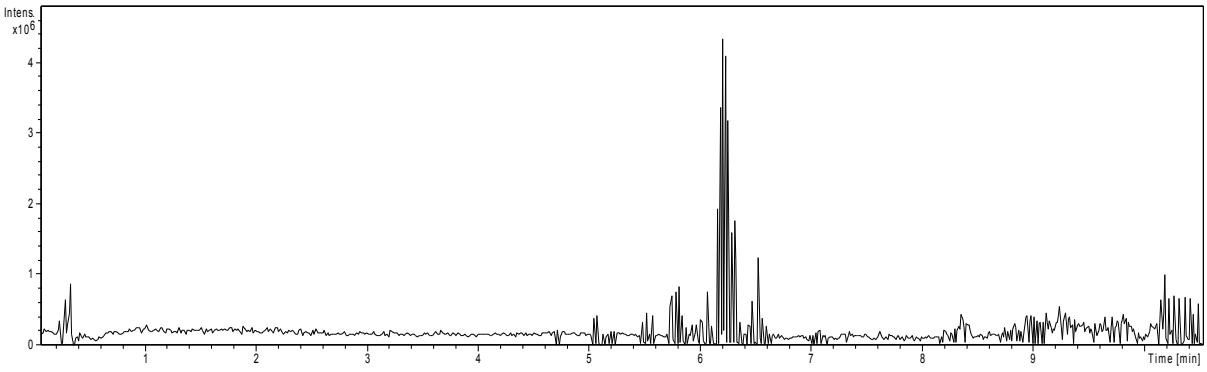

Figure 8B: Base peak chromatogram of purified IgG *N*-linked glycan. The large peak corresponds to the purified IgG *N*-linked glycan.

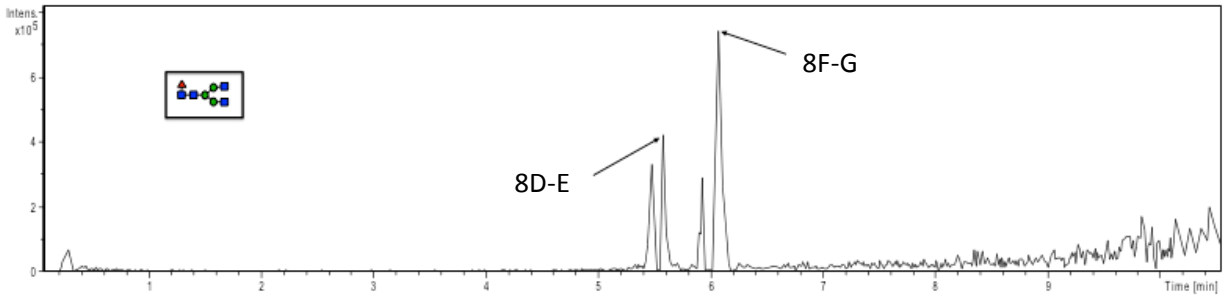

Figure 8C: EIC of a mass-to-charge ratio of 732 corresponding to IgG glycan in +2 charge state. There are two observable peaks, suggesting two species of the same molecule in our sample. Since the sample was not reduced, we believe these two peaks correspond to the alpha and beta anomers of the IgG *N*-linked glycan molecule. Within each big peak, there is a further division of two smaller peaks. There is not explanation for why this occurs.

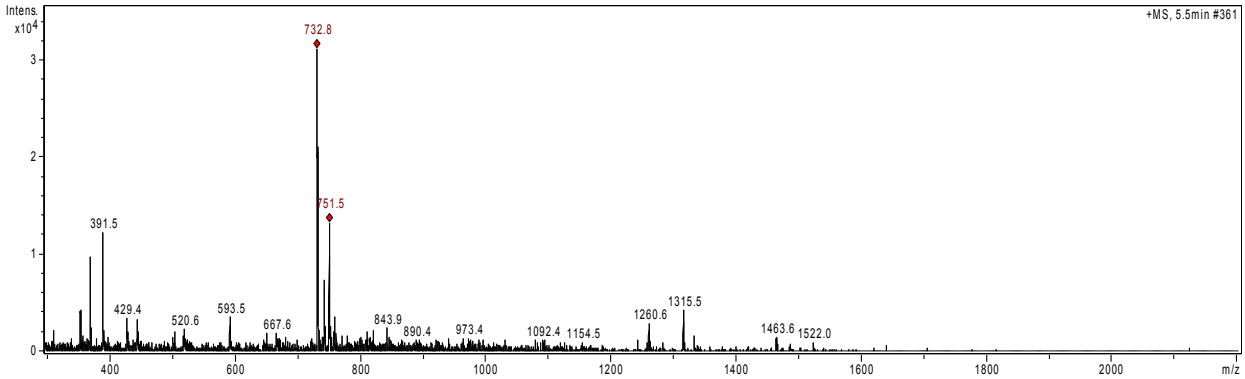

Figure 8D: MS of parent peak with a mass-to-charge ratio of 732.8, observed at approximately 5.5 minutes. This peak corresponds to the IgG glycan in a +2 charge state.

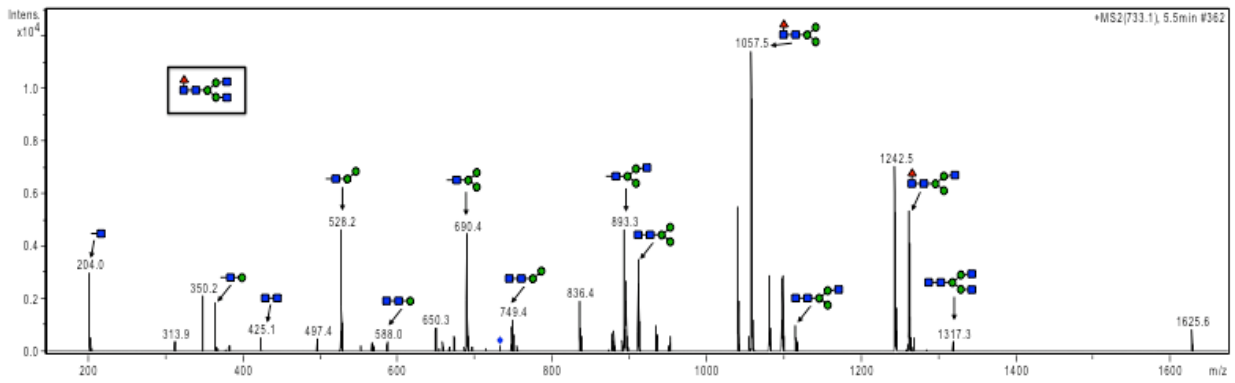

Figure 8E: MS/MS fragmentation pattern of parent peak with mass-to-charge ratio of 733.1 observed at approximately 5.5 minutes. We believe that both peaks are for the same molecule, which can be proven by comparing the fragmentation patterns of both peaks. The first peak was determined to be specific to the known IgG glycan molecule.

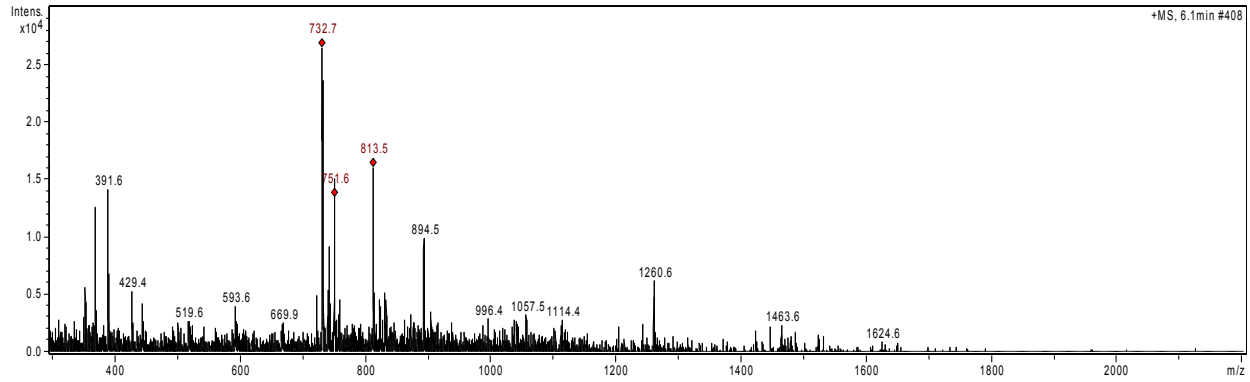

Figure 8F: MS of parent peak with a mass-to-charge ratio of 732.7, observed at approximately 6.1 minutes. This peak corresponds to the IgG glycan in a +2 charge state.

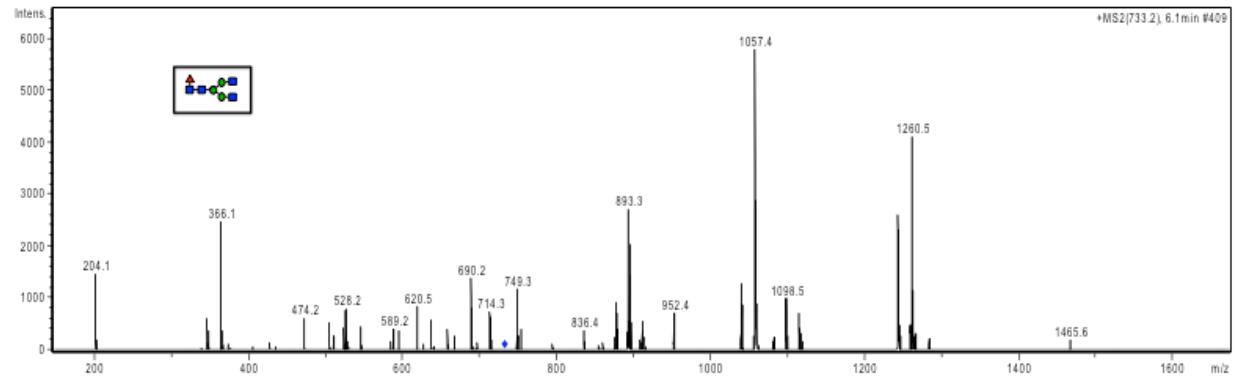

Figure 8G: MS/MS fragmentation pattern of parent peak with mass-to-charge ratio of 733.2 observed at approximately 6.1 minutes. This fragmentation pattern is from the molecule with the most intense peak seen on the EIC. It is also specific to the known IgG glycan molecules, and is an almost exact replica of the fragmentation pattern seen for the earlier-eluted molecule. This suggests that each peak corresponds to the same IgG *N*-linked glycan molecule.

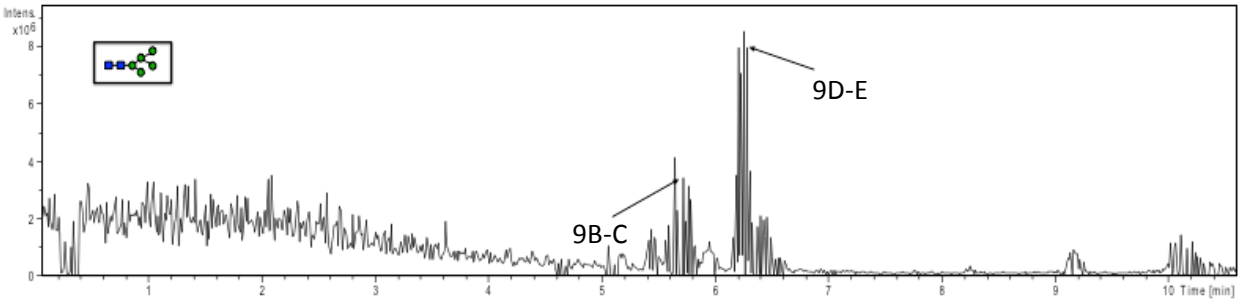

Figure 9A: BPC of *N*-linked glycans isolated from Lfng protein grown in Lec1 CHO cells. This chromatogram shows two prominent peaks, suggesting the presence of two different glycans. From our previous runs with IgG and $Man_9GlcNAc_2$ glycans, it is likely that both peaks corresponding to the same molecule in different anomeric conformations. This is proven by the similarity in fragmentation observed between molecules from both peaks.

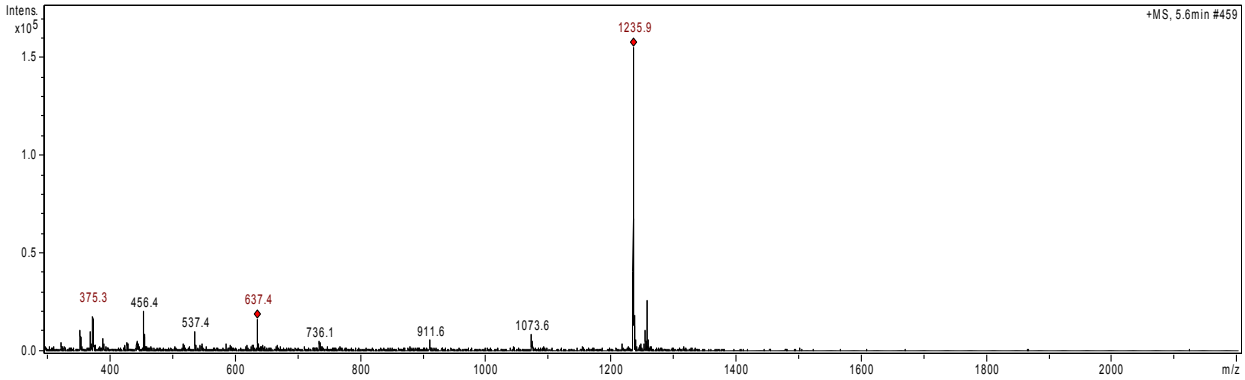

Figure 9B: MS of parent peak with a mass-to-charge ratio of 1235.9, observed at approximately 5.6 minutes. This peak corresponds to a preliminary Lfng *N*-linked glycan in the +1 charge state.

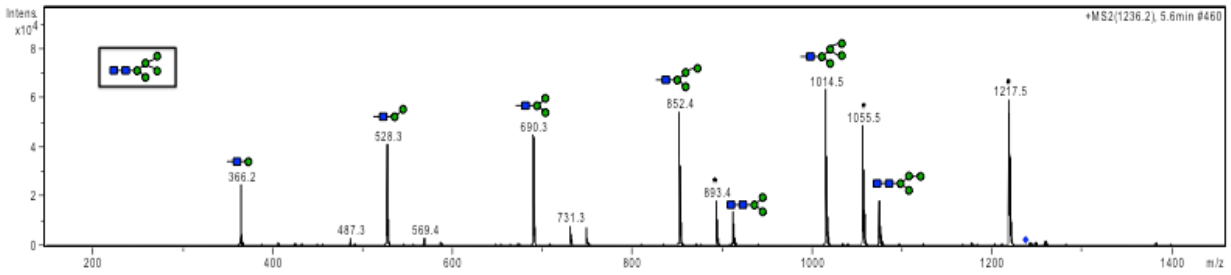

Figure 9C: MS/MS fragmentation pattern of parent peak with mass-to-charge ratio of 1236.2 observed at approximately 5.6 minutes. Analysis of this chromatogram allowed us to characterize a preliminary glycan structure that is abundant in this sample.

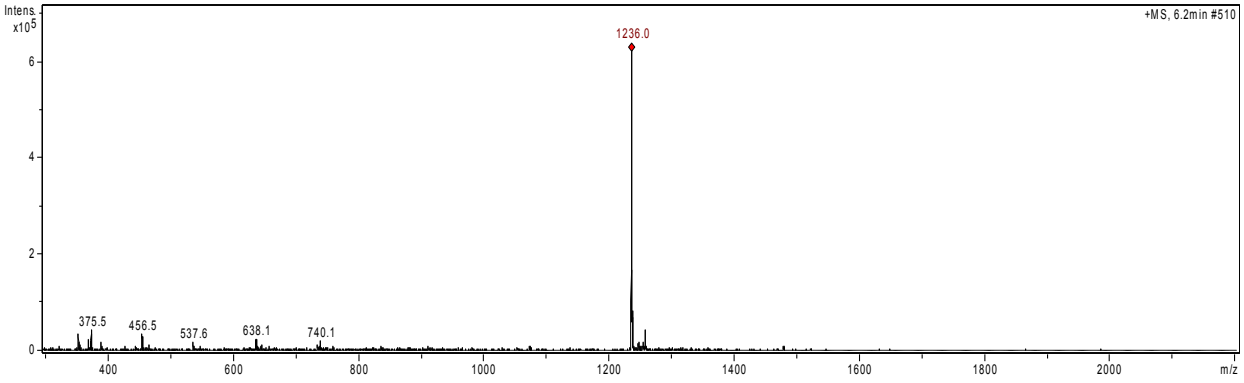

Figure 9D: MS of parent peak with a mass-to-charge ratio of 1236.0, observed at approximately 6.2 minutes. This peak corresponds to a preliminary Lfng *N*-linked glycan in the +1 charge state.

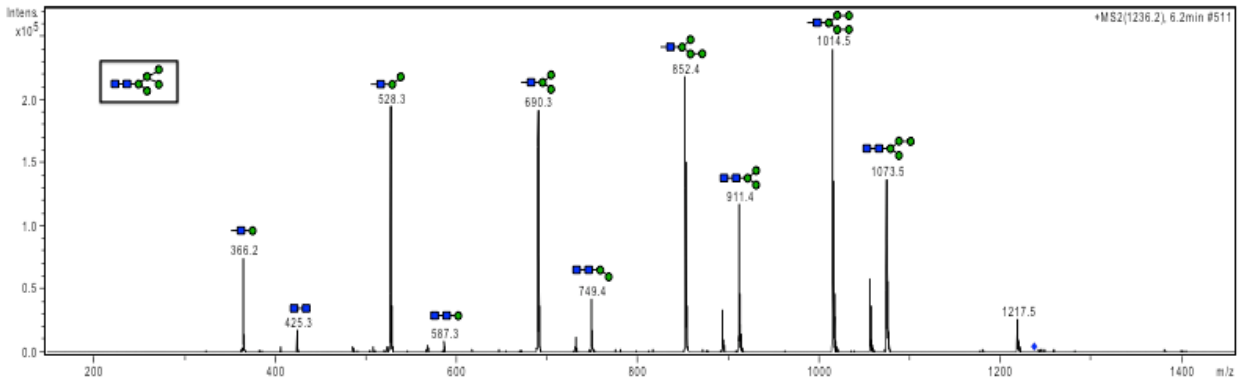

Figure 9E: MS/MS fragmentation pattern of parent peak with mass-to-charge ratio of 1236.2 observed at approximately 6.2 minutes. This pattern is very similar to the pattern observed from fragmentation of molecules from the earlier eluted peak, which suggests that they may be the same molecules. Analysis of the individual mass-to-charge ratios of each peak gave us the same structure predicted from the previous peak, giving us stronger evidence that this is the glycan structure attacked to Lfng.

Figure 9F: Preliminary Lfng *N*-linked glycan structures. The calculated molecular weight of the suspected Lfng *N*-linked glycan without a core fucose modification is 1234.42 Daltons. With core fucosylation, the molecular weight is predicted to be 1380.48 Daltons.

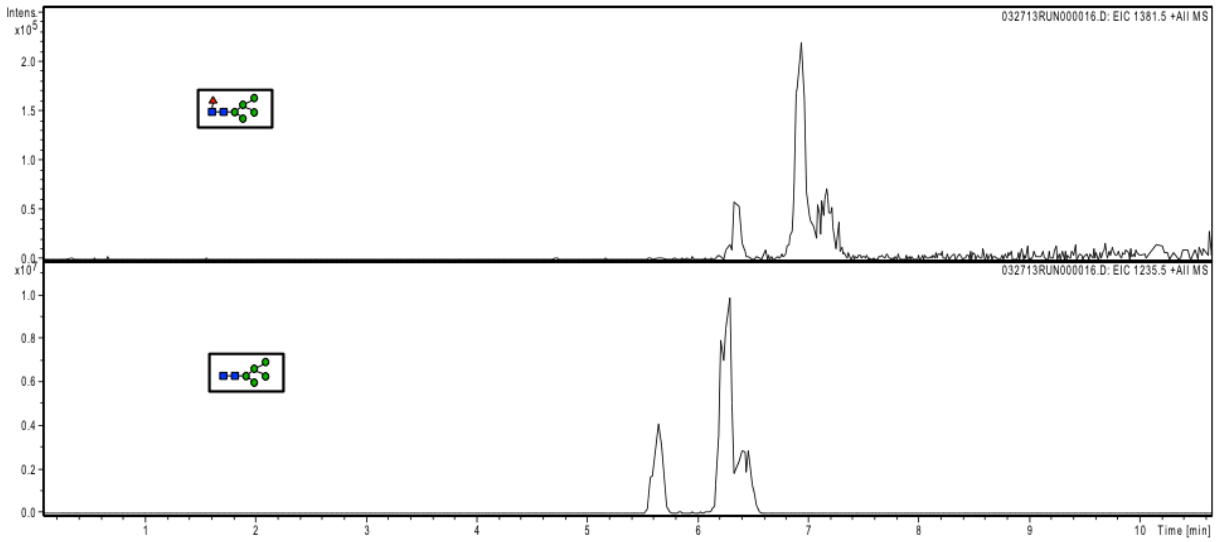

Figure 9G: Comparison between EIC of preliminary Lfng glycan structure with fucose modification (1381 m/z in the +1 charge state) and EIC of preliminary Lfng glycan structure without fucose modification (1236 m/z in the +1 charge state). The intensity of peaks from EIC at 1381 is much lower than that at 1236, making it difficult for us to analyze this molecule. This data suggests that the fucose-modified species is present in our sample, but in very low amounts. This agrees with the fact that our Lfng were grow in Lec1 CHO cells, a cell type that is unable to make hybrid or complex *N*-linked glycans due to a mutation in GlcNAcT-1.

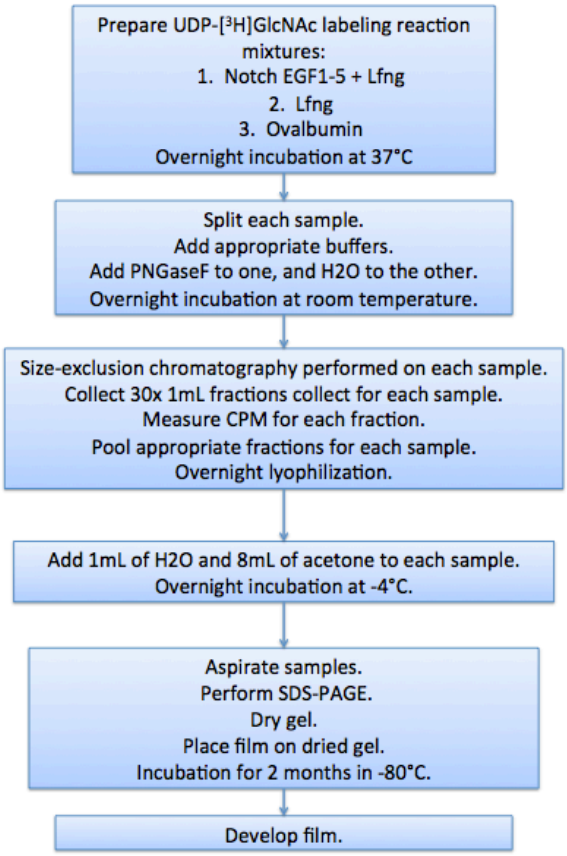

Figure 10A: Flowchart of individual steps taken to complete radioactivity assay. This method was used to test Lfng's ability to catalyze the addition of radioactive GlcNAc from UDP-**[^{3}H]**GlcNAc on to itself.

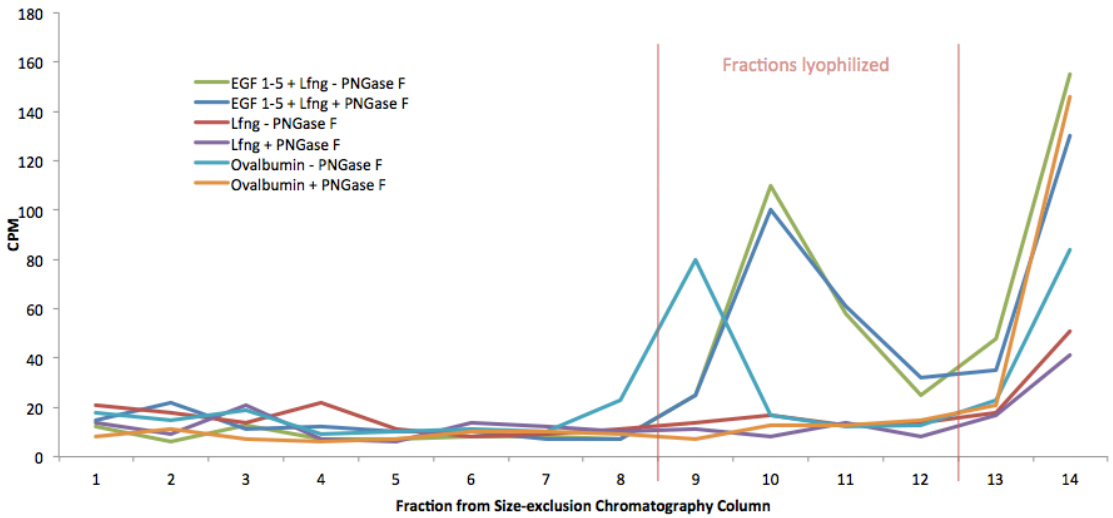

Figure 10B: Scintillation readings for aliquots of sample collected from size exclusion chromatography of samples with varying radioactivity assay reagents. The EGF1-5 is expected to be modified with the addition of radioactive GlcNAc, as is confirmed by our scintillation data (see legend). There is an unexpected spike in radioactivity for Ovalbumin, which remains unexplained. Ovalbumin is a positive control for PNGase F activity, and has no sites for GlcNAc modification. This experiment was done to test the ability for Lfng to catalyze the addition of radioactive GlcNAc on to itself, however no incorporation is evident from the scintillation data.

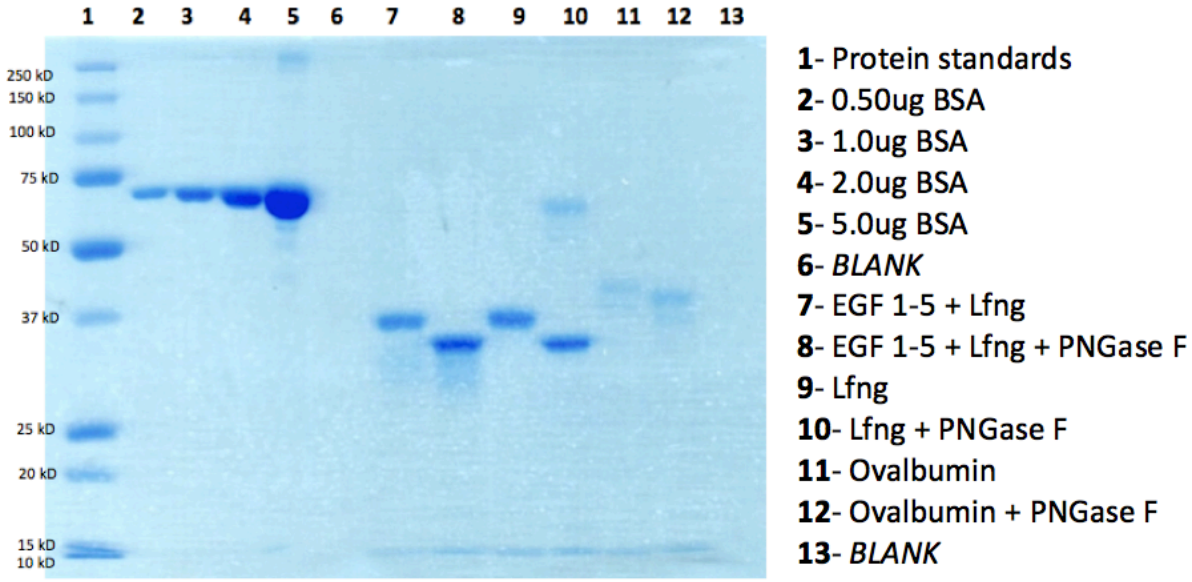

Figure 10C: Protein samples, from scintillation counter tests, purified and separated by SDS-PAGE. A total of 10 µg of substrate protein was added to each lane- comparison of BSA stain and protein stain suggests that a large amount of our protein was lost through the purification process. However, all of our protein is visible after staining. EGF1-5 is present in lanes 7 and 8 in the form of a smear, as expected. Lfng is also present in each of these lanes, as it is the enzyme used to modify EGF 1-5, thus allowing it to be the positive control for enzyme activity. Lanes 8 and 9 contain only Lfng. A shift is seen in these lanes, as the *N*-linked glycans are cleaved in lane 10 by the enzyme PNGase F. Lanes 11 and 12 had Ovalbumin, both clearly visible. Ovalbumin serves a positive control for PNGase F activity. There is a visible shift in bands, due to the cleavage of glycans in lane 12 by PNGase F.

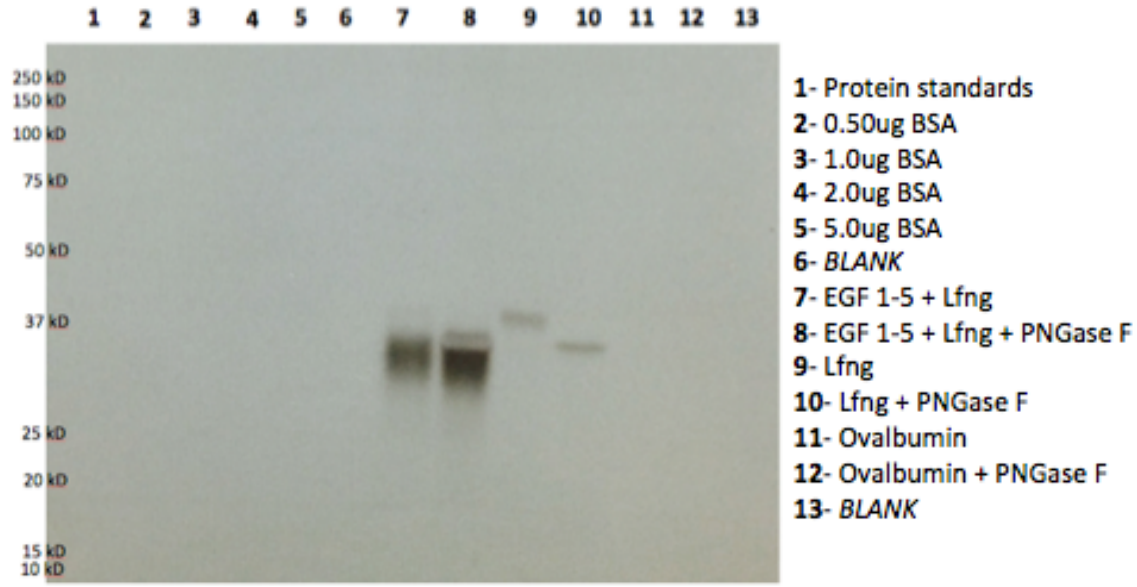

Figure 10D: SDS-PAGE gel dried and placed on an undeveloped film for two months. This autoradiograph was developed. The EGF 1-5 lanes reveals expected radioactive signal, while there is none observed in the Ovalbumin lanes. Both Lfng lanes, with and without Lfng treatment, reveal radioactivity. In the EGF 1-5 lane treated with PNGase F, there is a clear band overlapping the radioactive EGF 1-5 smear; this band runs at the same size as deglycosylated Lfng.

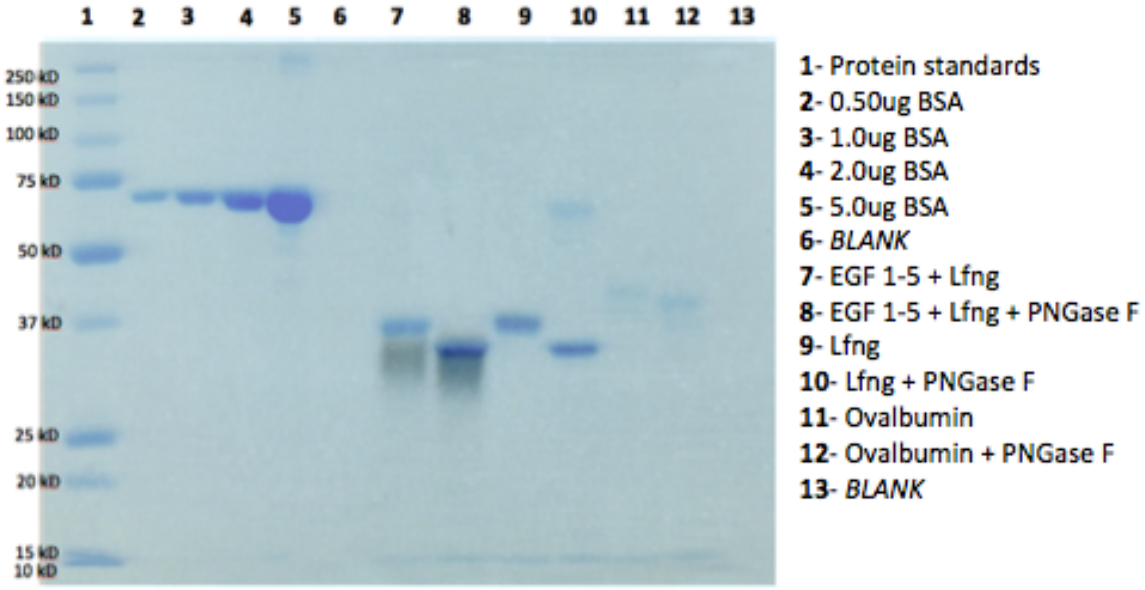

Figure 10E: Coomassie gel with protein sample (Fig. 10C) with autoradiograph (Fig. 10D) placed on top to reveal identities of radioactive signals. The Coomassie stained gel is 50% transparent in this image.

References

Acar, M., H. Jafar-Nejad, H. Takeuchi, A. Rajan, D. Ibrani, N. A. Rana, H. Pan, R. S. Haltiwanger and H. J. Bellen (2008). "Rumi is a CAP10 domain glycosyltransferase that modifies Notch and is required for Notch signaling." Cell **132**(2): 247-258.

Al-Shareffi, E., J. L. Chaubard, C. Leonhard-Melief, S. K. Wang, C. H. Wong and R. S. Haltiwanger (2013). "6-alkynyl fucose is a bioorthogonal analog for O-fucosylation of epidermal growth factor-like repeats and thrombospondin type-1 repeats by protein O-fucosyltransferases 1 and 2." Glycobiology **23**(2): 188-198.

Artavanis-Tsakonas, S., M. D. Rand and R. J. Lake (1999). "Notch signaling: cell fate control and signal integration in development." Science **284**(5415): 770-776.

Bruckner, K., L. Perez, H. Clausen and S. Cohen (2000). "Glycosyltransferase activity of Fringe modulates Notch-Delta interactions." Nature **406**(6794): 411-415.

Dexter, J. S. (1914). "The analysis of a case of continuous variation in Drosophila by a study of its linkage relations." The American Naturalist(48): 712-758.

Fortini, M. E. (2009). "Notch signaling: the core pathway and its posttranslational regulation." Dev Cell **16**(5): 633-647.

Guile, G. R., P. M. Rudd, D. R. Wing, S. B. Prime and R. A. Dwek (1996). "A rapid high-resolution high-performance liquid chromatographic method for separating glycan mixtures and analyzing oligosaccharide profiles." Anal Biochem **240**(2): 210-226.

Haltiwanger, R. S. and J. B. Lowe (2004). "Role of glycosylation in development." Annu Rev Biochem **73**: 491-537.

Harris, R. J. and M. W. Spellman (1993). "O-linked fucose and other post-translational modifications unique to EGF modules." Glycobiology **3**(3): 219-224.

Helenius, A. and M. Aebi (2004). "Roles of N-linked glycans in the endoplasmic reticulum." Annu Rev Biochem **73**: 1019-1049.

Irvine, K. and E. Wieschaus (1994). "Fringe, a Boundary-specific signaling molecule, mediates interactions between dorsal and ventral cells during Drosophila wing development. ." Cell **79**(4): 595-606.

Jafar-Nejad, H., J. Leonardi and R. Fernandez-Valdivia (2010). "Role of glycans and glycosyltransferases in the regulation of Notch signaling." Glycobiology **20**(8): 931-949.

Jarriault, S., C. Brou, F. Logeat, E. H. Schroeter, R. Kopan and A. Israel (1995). "A Signaling downstream of activated mammalian Notch." Nature **377**: 355-358.

Jensen, P. H., N. G. Karlsson, D. Kolarich and N. H. Packer (2012). "Structural analysis of N- and O-glycans released from glycoproteins." Nat Protoc **7**(7): 1299-1310.

Johnston, S. H., C. Rauskolb, R. Wilson, B. Prabhakaran, K. D. Irvine and T. F. Vogt (1997). "A family of mammalian Fringe genes implicated in boundary determination and the Notch pathway." Development **124**(11): 2245-2254.

Kang, P., Y. Mechref, I. Klouckova and M. V. Novotny (2005). "Solid-phase permethylation of glycans for mass spectrometric analysis." Rapid Commun Mass Spectrom **19**(23): 3421-3428.

Luo, Y. and R. S. Haltiwanger (2005). "O-fucosylation of notch occurs in the endoplasmic reticulum." J Biol Chem **280**(12): 11289-11294.

Mohr, O. L. (1919). "Character Changes Caused by Mutation of an Entire Region of a Chromosome in Drosophila." Genetics **4**(3): 275-282.

Moloney, D. J., V. M. Panin, S. H. Johnston, J. Chen, L. Shao, R. Wilson, Y. Wang, P. Stanley, K. Irvine, R. S. Haltiwanger and T. F. Vogt (2000). "Fringe is a glycosyltransferase that modifies Notch." Nature **406**: 369-375.

Rademacher, T. W., S. W. Homans, R. B. Parekh and R. A. Dwek (1986). "Immunoglobulin G as a glycoprotein." Biochem Soc Symp **51**: 131-148.

Rana, N. A. and R. S. Haltiwanger (2011). "Fringe benefits: functional and structural impacts of O-glycosylation on the extracellular domain of Notch receptors." Curr Opin Struct Biol **21**(5): 583-589.

Rodriguez-Esteban, C., J. W. Scwabe, J. De La Pena, B. Foys, B. Eshelman and J. C. Izpisua Belmonte (1997). "Radical fringe positions the apical ectodermal ridge at the dorsoventral boundary of the vertebrate limb." Nature **386**(6623): 360-366.

Schroeter, E. H., J. A. Kisslinger and R. Kopan (1998). "Notch-1 signaling requires ligand-induced proteolytic release of intracellular domain." Nature **393**(6683): 382-386.

Shi, S. and P. Stanley (2003). "Protein O-fucosyltransferase 1 is an essential component of Notch signaling pathways." Proceedings of the National Academy of Sciences of the United States of America **100**(9): 5234-5239.

Takeuchi, H., R. C. Fernandez-Valdivia, D. S. Caswell, A. Nita-Lazar, N. A. Rana, T. P. Garner, T. K. Weldeghiorghis, M. A. Macnaughtan, H. Jafar-Nejad and R. S. Haltiwanger (2011). "Rumi functions as both a protein O-glucosyltransferase and a protein O-xylosyltransferase." Proc Natl Acad Sci U S A **108**(40): 16600-16605.

van Tetering, G., P. van Diest, I. Verlaan, E. van der Wall, R. Kopan and M. Vooijs (2009). "Metalloprotease ADAM10 is required for Notch1 site 2 cleavage." The Journal of Biological Chemistry **285**(45): 31018-31027.

Varki, A., R. D. Cummings, J. D. Esko, H. H. Freeze, P. Stanley, C. R. Bertozzi, G. W. Hart and M. E. Etzler (2009). Essentials of Glycobiology. Cold Spring Harbor (NY), Cold Spring Harbor Press.

Wada, Y., P. Azadi, C. E. Costello, A. Dell, R. A. Dwek, H. Geyer, R. Geyer, K. Kakehi, N. G. Karlsson, K. Kato, N. Kawasaki, K. H. Khoo, S. Kim, A. Kondo, E. Lattova, Y. Mechref, E. Miyoshi, K. Nakamura, H. Narimatsu, M. V. Novotny, N. H. Packer, H. Perreault, J. Peter-Katalinic, G. Pohlentz, V. N. Reinhold, P. M. Rudd, A. Suzuki and N. Taniguchi (2007). "Comparison of the methods for profiling glycoprotein glycans—HUPO Human Disease Glycomics/Proteome Initiative multi- institutional study." Glycobiology **17**(4): 411-422.

Wharton, K. A., K. M. Johansen, T. Xu and S. Artavanis-Tsakonas (1985). "Nucleotide sequence from the neurogenic locus notch implies a gene product that shares homology with proteins containing EGF-like repeats." Cell **43**(3 Pt 2): 567-581.

Wuhrer, M., A. R. de Boer and A. M. Deelder (2009). "Structural glycomics using hydrophilic interaction chromatography (HILIC) with mass spectrometry." Mass spectrometry reviews **28**(8): 192-206.

Zhang, N. and T. Gridley (1998). "Defects in somite formation in lunatic fringe-deficient mice." Nature **394**(6691): 374-377.